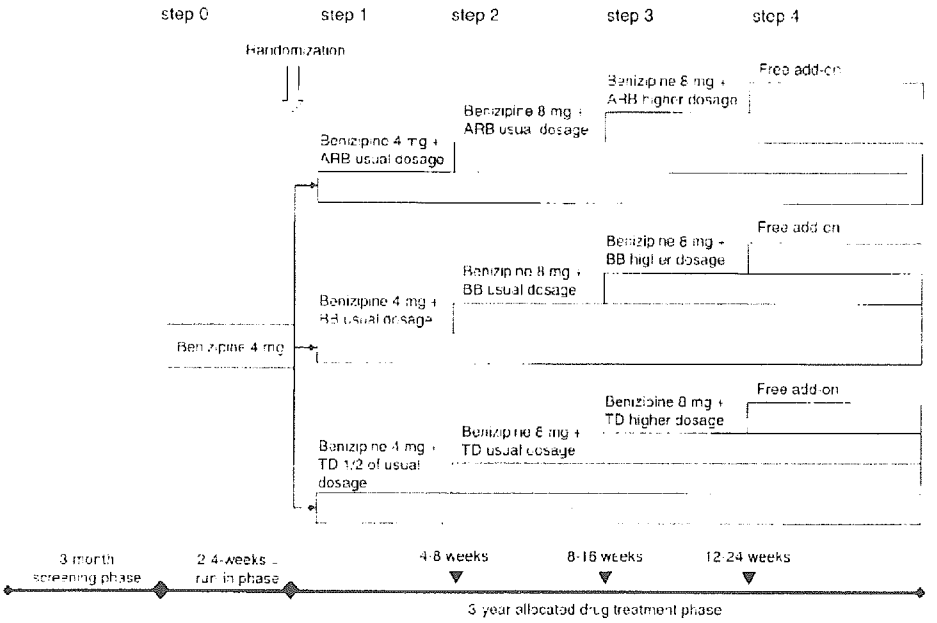

Fig. 1. *Outline of the design of the COPE trial. ARB, angiotensin receptor blockers; BB, β-blockers; TD, thiazide diuretics. "Free add-on" indicates that antihypertensive drugs other than those used for allocation—*i.e., *antihypertensive drugs other than calcium antagonists, angiotensin receptor blockers, β-blockers, or thiazide diuretics—can be added onto the drugs at step 4.*

the true effect of any intervention, all the collaborating investigators counsel their patients regarding the importance of the patients' adherence to the trial. In this way adverse event and clinical endpoint data continue to be collected on all patients. Patients withdrawn from the study drug during the treatment period may be switched to the other drugs or re-prescribed, if possible, at the investigator's discretion. If there is a need to start any therapy for any clinical indication during the study period, the investigator may prescribe additional therapy on top of the study drug. Drugs and dosages can be added at the investigator's discretion.

Endpoint Assessment

An Independent Endpoint Classification Committee will review and adjudicate cardiovascular events and all deaths and classify all potential cases without knowledge of assigned drugs according to criteria specified in the endpoint protocol. The classification of primary and secondary endpoints is shown in Table 3. For the review of the trial, the endpoint reports of the Endpoint Classification Committee will be sent to the Independent Data Monitoring Committee at 6-month intervals.

Adverse Events

All patients are questioned about adverse events at each follow-up visit. If a serious adverse event occurs, the investigators, at their discretion, may interrupt or discontinue the study drug. Both serious and non-serious adverse events are recorded, and the Safety Committee will review the data. The reports of the Safety Committee will be sent for review to the Independent Data Monitoring Committee at 6-month intervals.

Safety Considerations

The Independent Data Monitoring Committee, not involved in the administration of the trial, monitors all endpoints and medically serious and non-serious adverse events, and will perform interim analyses on the primary efficacy parameters at intervals throughout the study. The Independent Data Monitoring Committee receives safety reports from the Safety Committee and endpoint reports from the Endpoint Classification Committee at 6-month intervals, and will convene to review the trial. This Committee will have sole access to unblinded data and will inform the Steering Committee if there is a recommendation to discontinue the trial.

Statistical Considerations

Sample-Size Determination

The planned sample size (total 3,000, each arm 1,000) was determined mainly by considerations of feasibility. Regarding the proportion of patients attaining the target blood pressure levels, which is one of the primary endpoints, the

Table 3. Primary and Secondary Endpoints

1. Primary endpoints
   1) A composite of fatal and non-fatal cardiovascular events
      (1) Sudden death (acute onset and intrinsic death within 24 h)
      (2) Fatal or nonfatal stroke (new onset or recurrence)
      (3) Fatal or nonfatal myocardial infarction (new onset or recurrence), hospitalization due to unstable angina, new onset of heart failure (Class II, III, or IV), sudden cardiac death
      (4) New onset or worsening of peripheral arterial disease
      (5) New onset or worsening of renal failure (as indicated by a serum creatinine level that is at least doubled to over 2 mg/dl), serum creatinine ≥4.0 mg/dl, renal dialysis or renal transplantation
   2) Achievement of target blood pressure (systolic blood pressure < 140 mmHg and diastolic blood pressure < 90 mmHg)
2. Secondary endpoints
   (1) All-cause mortality
   (2) Death from cardiovascular events
   (3) Fatal and non-fatal cardiovascular events
   (4) Hospitalization due to heart failure
   (5) New onset of diabetes mellitus
   (6) Safety (adverse events and adverse drug reaction)

required sample size for detecting a 5% difference among treatment arms around the average proportion 50% (type I error, two sided $\alpha = 0.10$ with multiplicity adjustments; power $1-\beta = 0.90$) is about 620 for each arm, and thus the planned sample size is expected to have high statistical power. The required sample size for detecting a clinically significant difference in one of the primary endpoints, the incidence of cardiovascular events, with a high statistical power is huge (5,000–10,000 for each arm in the current situation), as will be illustrated later. Therefore, the objective of this trial is to identify the optimal combination of drugs based on the achievement of target blood pressure level, incidence of cardiovascular events, profile of major adverse drug reactions, and incidence of newly diagnosed diabetes. For three endpoints, besides incidence of cardiovascular events, sufficient statistical power is expected with a sample size greater than 600 per arm, and the current sample size (total 3,000) was selected to assure a high probability of selecting a better combination (if there are differences among arms in the incidence of vascular events), as described later. The results of this trial will be submitted to future meta-analyses of similar trials with the objective of comparing anti-hypertensive drug combinations, and the sample size used will protect against interactions between trial and treatment arms.

Based on recent Japanese clinical trials (*14*, *26*), the incidence of cardiovascular events in the patient population of this trial is expected to be around 20/1,000 person-years or around 15/1,000 person-years if the combination therapy is effective. The expected person-years and the expected number of events from the planned follow-up of 3,000 patients are approximately 11,000 and 165–220, respectively. On the other hand, the necessary number of events for detecting a clinically significant risk ratio of 1.2 (two sided $\alpha = 0.05$; $1-\beta = 0.90$) is 633 in an inferior arm. The necessary numbers of events for assuring the non-inferiority of the diuretic arm against the other two arms combined are 475 and 380 in each arm if the clinically acceptable limit of risk ratios are 1.2 and 1.25, respectively (under the assumption of the diuretic arm being similarly effective). These numbers are far from those expected from the current settings of this trial. Therefore, we calculated the number of events necessary to assure the high probability in such a way that the results of a truly better arm will not be overtaken by those of a truly inferior arm: the necessary number is calculated as 70–80 in each arm if the clinically significant risk ratio is defined as 1.2 and the probability is set to 0.95 (taking account of a multiplicity of 3 comparisons). This number is attainable by the current settings of this trial.

Statistical Analysis

The incidence of cardiovascular events, which is one of the two primary endpoints, is analyzed using the methods of time-to-event analysis (*27*). The cumulative incidence rates are calculated using the Kaplan-Meier method defining the random allocation date as the starting point. The comparison among treatment arms is conducted using the log-rank test. If the overall p-value is less than 0.10, then a pair-wise comparison is calculated for the interpretation. The logarithm of hazard ratio and its 95% confidence interval are calculated from the log-rank scores and the Cox regression with adjustment of important prognostic factors for each comparison of drug combinations. Based on these statistics, Bayesian posterior probabilities for superiority and non-inferiority among treatment arms are calculated: the limit of clinical equivalence is set as 1/1.2–1.2.

The other primary endpoint, the cumulative proportion of patients attaining the target blood pressure levels, is summarized using the Kaplan-Meier method and compared by the generalized Wilcoxon test. All statistical tests will be two-sided with values of $p < 0.05$ indicating statistical significance unless otherwise stated.

Organizational Structure

The organization and the members of the various committees of the COPE trial are given in Appendix. The Principal Study Coordinators and the Steering Committee have responsibility for the general design and administration of the study. This includes the responsibility for reviewing and implementing recommendations from the Independent Data Monitoring Committee, for protocol changes, and for premature termination of the study because of lack of treatment efficacy or early demonstration of benefit. Together, these activities will ensure that the trial is progressing properly, efficiently, and in accordance with protocol. The Protocol Committee has responsibility for the study design and protocol changes. The Safety Committee is responsible for the evaluation of adverse events and for recommendations to the Steering Committee if a serious adverse event occurs. The Endpoint Classification Committee is responsible for evaluation of the primary and secondary endpoints. This committee consists of a chair, 2 cardiologists, 2 nephrologists, and 2 neurologists. The Independent Data Monitoring Committee is responsible for overseeing the welfare of the patients enrolled in the trial, reviewing the compliance and trial progress at specified intervals as requested by the Executive Committee, and making recommendations to the Executive Committee should any problems arise. The Study Statistician is responsible for designing the statistical analysis plan and determining the validity of the analysis results. The Coordinating Center is responsible for organizing the Committees and will analyze the study data. The Coordinating Center liaises with the COPE Trial Data Center, which is responsible for patient registry and data management.

Discussion

Hypertension is a major risk factor for cardiovascular diseases. It is evident that most patients with moderate or severe hypertension require two or more antihypertensive agents to achieve appropriate blood pressure control (*3*, *10*, *11*). The recent guidelines for hypertension in the USA and Europe recommend using a combination of two agents as an initial therapy in patients with moderate or severe hypertension (*3*, *10*). An obvious disadvantage of initiating with two drugs, even if at a low dose, is the potential for exposing the patient to an unnecessary agent, but the advantages of combination therapies are: 1) by using two drugs with different mechanisms of action, it is more likely that the blood pressure will be controlled and complications prevented; 2) by using combinations, both the first and second drugs can be given in the low-dose range, which is more likely to be free of side-effects, thus optimizing compliance (*10*). It is likely that some combinations of antihypertensive agents are more clinically effective than others; however, despite the recommendation of the major hypertension treatment guidelines that combination therapy be used as a first-line treatment, only a limited number of reports have attempted to identify which combinations are best for antihypertensive treatments and for the prevention of cardiovascular disease (*3*, *10*). Thus, it is clear that the next challenge will be to determine which combination regimens will provide the greatest cardiovascular benefits for patients with hypertension.

The seventh report of the Joint National Committee on Prevention, Detection, Evaluation, and Treatment of High Blood Pressure (JNC 7) cites 30 combination drugs for hypertension (*3*). Most of these combination drugs consist of an antihypertensive and a diuretic. In Japan, however, calcium antagonists are the most widely prescribed antihypertensives (*21*). When a questionnaire survey was administered to Japanese clinical specialists in hypertension to gauge their opinions on the 1999 revised version of the Guidelines for Hypertension in the Elderly, 65% of the respondents selected long-acting calcium antagonists, ACE inhibitors, and low-dose diuretics as first-line agents for the treatment of hypertension without complications in the elderly (*28*). In addition, it was reported that the combination of a calcium antagonist with an ACE inhibitor or angiotensin receptor blocker was their first-choice drug combination (*20*). It is generally considered that the most rational combinations consist of a calcium antagonist and either an ACE inhibitor, an angiotensin receptor blocker, a β-blocker, or a thiazide diuretic (*10*). Therefore, it is very useful and important to compare the efficacy of each calcium antagonist-based combination in Japan.

In the COPE trial, the calcium antagonist benidipine was selected as the initial drug for combination therapy for the treatment of essential hypertension in Japan. Several mega-trials and meta-analyses have confirmed that calcium antagonists are as effective as other agents in reducing overall morbidity and mortality in hypertensive patients, and that they also lower blood pressure (*4*, *28*, *29*). It has also been demonstrated that calcium antagonists decrease the risk of stroke more effectively than other treatments in patients with essential hypertension (*30*). Benidipine is well tolerated at a dose of 4–8 mg/day and is an effective treatment for patients with mild to moderate hypertension (*24*). In addition, it is suggested that combination therapy with benidipine and an angiotensin receptor blocker decreases blood pressure more effectively than either drug alone and may be expected to add benefits to the treatment of hypertension (*31*, *32*).

To ensure data quality, efficiently enroll a sufficient number of patients, and improve administration of the trial, clinical research coordinators from the site management organization will provide the collaborating investigators with technical assistance in data collection and report preparation, thereby reducing their workload.

In conclusion, the COPE trial is an important study that will help to clarify the questions of which antihypertensive combination confers the best protection against cardiovascular mortality and morbidity, and which antihypertensive combination best achieves the target blood pressure.

Appendix

The Combination Therapy of Hypertension to Prevent Cardiovascular Events Trial Group

Principal Study Coordinators: T. Ogihara, T. Saruta.

Steering Committee: M. Matsuzaki (Chairman), K. Kikuchi, S. Itoh, H. Matsuoka, H. Suzuki, T. Fujita, J. Higaki, T. Etoh, C. Tei, A. Kamiya.

Protocol Committee: H. Matsuoka (Chairman), K. Shimamoto, H. Kumagai, H. Rakugi, S. Takishita, Y. Ohashi, S. Umemoto.

Safety Committee: N. Suzuki (Chairman), S. Nogawa, T. Yoshikawa, K. Yumura, K. Utsunomiya.

Endpoint Classification Committee: K. Shimada (Chairman), K. Kario, K. Kitagawa, H. Makino, M. Matsumoto, K. Hayashi, M. Kawana.

Independent Data Monitoring Committee: K. Abe (Chairman), M. Fujishima, K. Otsuka, Y. Ohashi, K. Tanabe.

Study Statistician: Y. Ohashi.

Coordinating Center: EBM Office, Pharmaceutical Clinical Research Center, Yamaguchi University Hospital.

References

1. Kannel WB: Blood pressure as a cardiovascular risk factor: prevention and treatment. *JAMA* 1996; **275**: 1571–1576.
2. Gorelick PB, Sacco RL, Smith DB, *et al*: Prevention of a first stroke: a review of guidelines and a multidisciplinary consensus statement from the National Stroke Association. *JAMA* 1999; **281**: 1112–1120.
3. Chobanian AV, Bakris GL, Black HR, *et al*: Seventh report of the Joint National Committee on Prevention, Detection, Evaluation, and Treatment of High Blood Pressure. *Hypertension* 2003; **42**: 1206–1252.
4. Staessen JA, Wang JG, Thijs L: Cardiovascular protection and blood pressure reduction: a meta-analysis. *Lancet* 2001; **358**: 1305–1315.
5. Turnbull F: Effects of different blood-pressure-lowering regimens on major cardiovascular events: results of prospectively-designed overviews of randomised trials. *Lancet* 2003; **362**: 1527–1535.
6. Yamori Y, Nara Y, Mizushima S, Sawamura M, Horie R: Nutritional factors for stroke and major cardiovascular diseases: international epidemiological comparison of dietary prevention. *Health Rep* 1994; **6**: 22–27.
7. Levi F, Lucchini F, Negri E, La Vecchia C: Trends in mortality from cardiovascular and cerebrovascular diseases in Europe and other areas of the world. *Heart* 2002; **88**: 119–124.
8. Ueshima H, Zhang XH, Choudhury SR: Epidemiology of hypertension in China and Japan. *J Hum Hypertens* 2000; **14**: 765–769.
9. Koshy S, Bakris GL: Therapeutic approaches to achieve desired blood pressure goals: focus on calcium channel blockers. *Cardiovasc Drugs Ther* 2000; **14**: 295–301.
10. European Society of Hypertension–European Society of Cardiology Guidelines Committee: 2003 European Society of Hypertension–European Society of Cardiology guidelines for the management of arterial hypertension. *J Hypertens* 2003; **21**: 1011–1053.
11. Whitworth JA, World Health Organization, International Society of Hypertension Writing Group: 2003 World Health Organization (WHO)/International Society of Hypertension (ISH) statement on management of hypertension. *J Hypertens* 2003; **21**: 1983–1992.
12. Japanese Society of Hypertension Guidelines Subcommittee for the Management of Hypertension: Guidelines for the management of hypertension for general practitioners. *Hypertens Res* 2001; **24**: 613–634.
13. Gong L, Zhang W, Zhu Y, *et al*: Shanghai trial of nifedipine in the elderly (STONE). *J Hypertens* 1996; **14**: 1237–1245.
14. National Intervention Cooperative Study in Elderly Hypertensives Study Group: Randomized double-blind comparison of a calcium antagonist and a diuretic in elderly hypertensives. *Hypertension* 1999; **34**: 1129–1133.
15. ALLHAT Officers and Coordinators for the ALLHAT Collaborative Research Group: Major outcomes in high-risk hypertensive patients randomized to angiotensin-converting enzyme inhibitor or calcium channel blocker vs diuretic: the Antihypertensive and Lipid-Lowering Treatment to Prevent Heart Attack Trial (ALLHAT). *JAMA* 2002; **288**: 2981–2997.
16. Yamamoto Y, Sonoyama K, Matsubara K, *et al*: The status of hypertension management in Japan in 2000. *Hypertens Res* 2002; **25**: 717–725.
17. Japanese Society of Hypertension Guidelines Subcommittee for the Management of Hypertension: Guidelines for the Management of Hypertension 2004. Tokyo, Life Science Publishing Co., Ltd., 2004, pp 4–6.
18. Hozawa A, Ohkubo T, Kikuya M, *et al*: Blood pressure control assessed by home, ambulatory and conventional blood pressure measurements in the Japanese general population: the Ohasama study. *Hypertens Res* 2002; **25**: 57–63.
19. Law MR, Wald NJ, Morris JK, Jordan RE: Value of low dose combination treatment with blood pressure lowering drugs: analysis of 354 randomised trials. *BMJ* 2003; **326**: 1427.
20. Saito I, Kawabe H, Tsujioka M, Hirose H, Shibata H: Trends in pharmacologic management of hypertension in Japan one year after the publication of the JSH 2000 guidelines. *Hypertens Res* 2002; **25**: 175–178.
21. Saruta T: Current status of calcium antagonists in Japan. *Am J Cardiol* 1998; **82**: 32R–34R.
22. Hansson L, Hedner T, Dahlof B: Prospective randomized open blinded end-point (PROBE) study. A novel design for intervention trials. Prospective Randomized Open Blinded End-Point. *Blood Press* 1992; **1**: 113–119.
23. Kalke S, Shah BV, Nair KG, Gala D, Sood OP, Bagati A: Clinical trial of benidipine in mild to moderate hypertension. *J Assoc Physicians India* 1999; **47**: 195–197.
24. Hoshide S, Kario K, Mitsuhashi T, Ikeda U, Shimada K: Is there any difference between intermediate-acting and long-acting calcium antagonists in diurnal blood pressure and autonomic nervous activity in hypertensive coronary artery disease patients? *Hypertens Res* 2000; **23**: 7–14.
25. Nomura M, Nakaya Y, Uemura E, *et al*: Effects of benidipine hydrochloride on autonomic nervous activity in hypertensive patients with high- and low-salt diets. *Arzneimittelforschung* 2003; **53**: 314–320.

26. Study Group on Long-Term Antihypertensive Therapy: A 12-month comparison of ACE inhibitor and CA antagonist therapy in mild to moderate essential hypertension—the GLANT Study. *Hypertens Res* 1995; **18**: 235–244.
27. Pocock SJ, Simon R: Sequential treatment assignment with balancing for prognostic factors in the controlled clinical trial. *Biometrics* 1975; **31**: 103–115.
28. Ogihara T, Morimoto S, Okaishi K, *et al*: Questionnaire survey on the Japanese guidelines for treatment of hypertension in the elderly: 1999 revised version. *Hypertens Res* 2002; **25**: 69–75.
29. Julius S, Kjeldsen SE, Weber M, *et al*: Outcomes in hypertensive patients at high cardiovascular risk treated with regimens based on valsartan or amlodipine: the VALUE randomised trial. *Lancet* 2004; **363**: 2022–2031.
30. Angeli F, Verdecchia P, Reboldi GP, *et al*: Calcium channel blockade to prevent stroke in hypertension: a meta-analysis of 13 studies with 103,793 subjects. *Am J Hypertens* 2004; **17**: 817–822.
31. Yao K, Sato H, Sonoda R, Ina Y, Suzuki K, Ohno T: Effects of benidipine and candesartan on kidney and vascular function in hypertensive Dahl rats. *Hypertens Res* 2003; **26**: 569–576.
32. Yao K, Sato H, Ina Y, Suzuki K, Ohno T, Shirakura S: Renoprotective effects of benidipine in combination with angiotensin II type 1 receptor blocker in hypertensive Dahl rats. *Hypertens Res* 2003; **26**: 635–641.

Regeneration of Infarcted Myocardium by Intramyocardial Implantation of Ex Vivo Transforming Growth Factor-β–Preprogrammed Bone Marrow Stem Cells

Tao-Sheng Li, MD, PhD; Masanori Hayashi, MD; Hiroshi Ito, MD, PhD; Akira Furutani, MD, PhD; Tomoaki Murata, PhD; Masunori Matsuzaki, MD, PhD; Kimikazu Hamano, MD, PhD

Background—Recent studies have shown that bone marrow–derived stem cells differentiate into the phenotype of cardiomyocytes in vivo and in vitro. We tried to regenerate infarcted myocardium by implanting ex vivo transforming growth factor (TGF)-β–preprogrammed CD117 (c-kit)–positive ($CD117^+$) stem cells intramyocardially.

Methods and Results—$CD117^+$ cells were isolated from the bone marrow mononuclear cells of GFP-transgenic or normal C57/BL6 mice. The myogenic differentiation of $CD117^+$ cells was achieved by cultivation with TGF-β. Using an acute myocardial infarction model, we also tried to regenerate infarcted myocardium by implanting untreated (newly isolated) or preprogrammed (24 hours of cultivation with 5 ng/mL TGF-β_1) $CD117^+$ cells intramyocardially. TGF-β increased the cellular expression of myosin, troponins, connexin-43, GATA-4, and NKx-2.5, which suggested that it induced the myogenic differentiation of $CD117^+$ cells. Compared with the effects of PBS injection only, the microvessel density in the infarcted myocardium was increased significantly 3 months after the implantation of either TGF-β–preprogrammed or untreated $CD117^+$ cells. Moreover, many of the TGF-β–preprogrammed $CD117^+$ cells were stained positively for myosin, whereas few of the untreated $CD117^+$ cells were. Histological analysis revealed newly regenerated myocardium in the left ventricular anterior wall after the implantation of TGF-β–preprogrammed cells but not untreated cells. Furthermore, the left ventricular percent fraction shortening was significantly higher after the implantation of TGF-β–preprogrammed cells than after the implantation of untreated $CD117^+$ cells.

Conclusions—TGF-β conducted the myogenic differentiation of $CD117^+$ stem cells by upregulating GATA-4 and NKx-2.5 expression. Therefore, the intramyocardial implantation of TGF-β–preprogrammed $CD117^+$ cells effectively assisted the myocardial regeneration and induced therapeutic angiogenesis, contributing to functional cardiac regeneration. (***Circulation.*** **2005;111:2438-2445.)**

Key Words: stem cells ■ myocardial infarction ■ regeneration ■ transforming growth factors

Experimental studies have shown that the intramyocardial implantation of various cells, including fetal cardiomyocytes, embryonic stem cell–derived cardiomyocytes, myoblasts, and bone marrow stem cells, offers a potentially effective method of repairing injured myocardium.[1–7] Bone marrow stem cells have become one of the most focused upon cell sources for repairing injured myocardium, because bone marrow–derived mesenchymal stem cells can differentiate into the phenotype of cardiomyocytes in vivo and in vitro.[7,8] Furthermore, recent studies have shown that ex vivo pretreatment of bone marrow–derived mesenchymal stem cells with 5-azacytidine induces myogenic differentiation and that the implantation of 5-azacytidine-treated cells has better potential for regenerating injured myocardium and improving cardiac function than the implantation of untreated cells.[6] Despite these promising results, the molecular mechanisms underlying myogenic differentiation from bone marrow stem cells remain poorly understood. To achieve effective regeneration of injured myocardium, it is important to find a more physiological way of improving the in situ myogenic differentiation of implanted bone marrow stem cells.

See p 2416

Transforming growth factor-β_1 (TGF-β_1) is a multifunctional cytokine involved in the differentiation, growth, and survival of various cells.[9] Recent investigations have shown that bone morphogenetic proteins, a subset of the transforming growth factor superfamily, promote cardiogenesis in vertebrate embryos.[10,11] One study demonstrated that exogenous TGF-β, or bone morphogenetic protein, increased the expression of cardiac transcription factors in embryonic stem cells and promoted the cardiac differentiation of embryonic

Received June 18, 2004; revision received September 14, 2004; November 23, 2004.

From the Divisions of Cardiovascular Surgery (T.L., M.H., H.I., A.F., K.H.) and Medicine (M.M.), Department of Medical Bioregulation, and Institute of Laboratory Animals (T.M.), Yamaguchi University School of Medicine, Ube, Yamaguchi, Japan.

Correspondence to Kimikazu Hamano, MD, PhD, Division of Cardiovascular Surgery, Department of Medical Bioregulation, Yamaguchi University School of Medicine, 1-1-1 Minami-Kogushi, Ube, Yamaguchi, Japan 755-8505.

Circulation **is available at http://www.circulationaha.org** **DOI: 10.1161/01.CIR.0000167553.49133.81**

stem cells.[12] Therefore, we speculated that TGF-β can conduct the myogenic differentiation of bone marrow stem cells and that ex vivo TGF-β pretreatment of bone marrow stem cells will increase their potential for functional cardiac regeneration after implantation.

We conducted this study to investigate whether TGF-β_1 could induce the myogenic differentiation of CD117$^+$ bone marrow stem cells in vitro. Moreover, we tried to achieve functional cardiac regeneration by implanting ex vivo TGF-β_1–preprogrammed CD117$^+$ stem cells using an acute myocardial infarction mouse model.

Methods

Animals

C57BL6/Tg14 (act-EGFP) OsbY01 mice were kindly provided by Masaru Okabe (Genome Research Center, Osaka University, Osaka)[13] and bred in the Animal Center of Yamaguchi University. Male C57BL/6 mice were purchased from Japan SLC (Shizuoka, Japan). All experiments were approved by the Institutional Animal Care and Use Committee of Yamaguchi University.

Isolation and Culture of Bone Marrow–Derived CD117$^+$ Stem Cells

CD117$^+$ cells were obtained by sorting, using the magnetic cell sorting (MACS) system (Miltenyi Biotec) as described previously.[14] Briefly, bone marrow mononuclear cells collected from the femur and tibia of mice were incubated with PE-conjugated anti-mouse CD117 (c-kit) antibody (Bioscience) for 30 minutes on ice. After washing with PBS, cells were incubated with anti-PE microbeads (Miltenyi Biotec) for 20 minutes. CD117$^+$ cells were separated by passing a MACS column. The purity of the CD117$^+$ cells collected by the MACS was ≈90%, and the viability was >99%. These purified CD117$^+$ cells expressed ≈8% to 20% of the lineage markers (Gr-1, MAC-1, B220, and TER119), 60% CD34, and 40% Sca-1.

Newly isolated CD117$^+$ cells were suspended in RPMI 1640 medium with a supplement of 15% FBS, then seeded in a 25-mm^2 flask or on 4-well chamber culture slides (Nalge Nunc International) coated with 0.2 mg/mL fibronectin (Sigma). Cells were cultured at 37°C with 0, 1, 5, or 100 ng/mL TGF-β_1. To detect the myogenic and osteoblast differentiation of CD117$^+$ cells induced by TGF-β_1, immunostaining was performed with mouse anti-myosin, ventricular heavy chain α/β monoclonal antibody (Chemicon Inc) and goat anti-mouse osteocalcin (Chemicon Inc), followed by incubation with FITC or R-PE–conjugated secondary antibodies, after 3 and 7 days of cultivation.[11]

Reverse Transcription–Polymerase Chain Reaction

Total RNA was extracted from freshly isolated CD117$^+$ cells or CD117$^-$ cells after 1, 3, and 7 days of culture by use of an RNA extraction kit (Omega Bio-Tek Inc). Reverse transcriptase–polymerase chain reaction (RT-PCR) was performed with an RNA PCR Kit (Takara) according to the manufacturer's instructions. The primers for RT-PCR were as follows: β-myosin heavy chain (528 bp): sense, 5′-GATCACCAACAACCCCTACG-3′; antisense, 5′-ATGCAGAGCTGCTCAAAGC-3′; cardiac troponin I (167 bp): sense, 5′-TCTCTACCTCTGGAGATCAGCATGG-3′; antisense, 5′-TGAAGTTTTCTGGAGGCGGAG-3; cardiac troponin T (416 bp): sense, 5′-AGGCGCTGATTGAGGCTCAC-3′; antisense, 5′-ATAGATGCTCTGCCACAGC-3′; connexin-43 (172 bp): sense, 5′-TTGACTTCAGCCTCCAAGG-3′; antisense, 5′-AATGAACAGCACCGACAGC-3′; GAPDH (861 bp): sense, 5′-CGGATTTGGTCGTATTGG-3′; antisense, 5′-TCAAAGGTGGAGGAGTGG-3′. PCR reactions were performed under the following conditions: 1 cycle at 94°C for 5 minutes, followed by 35 cycles at 94°C for 1 minute, 60°C for 1 minute, and 72°C for 1 minute. The PCR products were size-fractionated by 2% agarose gel electrophoresis.

Western Blot Analysis

Total protein was collected from freshly isolated CD117$^+$ cells or CD117$^-$ cells after 1 and 3 days of culture with or without the addition of 5 ng/mL TGF-β_1. The expression of GATA-4 and Nkx2.5, 2 important cardiac transcription factors, was measured by Western blot analysis using polyclonal antibodies against GATA-4 and Nkx2.5 (Santa Cruz), as described previously.[15]

Alkaline Phosphatase Activity Assay

To observe the osteoblast differentiation of CD117$^+$ cells, alkaline phosphatase (ALP) activity was determined as described by Uchimura et al.[16] Briefly, cells were collected after 1, 3, and 7 days of culture, then washed twice with PBS (−). The cell suspension was homogenized and sonicated, after which 20 μL of the sonicated cell suspension was used for DNA quantification. To measure the ALP activity, another sonicated cell suspension was centrifuged at 10 000 rpm for 1 minute at 4°C. An aliquot (20 μL) of the supernatant was assayed for ALP activity using p-nitrophenyl phosphate substrate (Zymed Laboratories Inc). The activity was represented by p-nitrophenol, which was released after incubation for 30 minutes at 37°C. ALP activity was compared with that of freshly collected cells and used for statistical analysis.

Myocardial Infarction Model and Intramyocardial Implantation of CD117$^+$ Cells

A myocardial infarction model was established in C57/BL6 mice as described previously.[3,15] After general anesthesia and tracheal intubation with a 20-gauge intravenous catheter, mice were artificially ventilated with room air (Harvard Apparatus Co) at 80 breaths per minute. We performed a left thoracotomy through the fourth intercostal space and ligated the left anterior descending artery with 9-0 Prolene under direct vision. The mice were then randomly given an intramyocardial injection with a 31-gauge needle in the infarction area at 4 points, with one of the following: 10 μL PBS (PBS group, n=20), 5×10^4 newly isolated CD117$^+$ cells (untreated group, n=34), or 5×10^4 CD117$^+$ cells preprogrammed with 5 ng/mL TGF-β_1 for 24 hour (preprogrammed group, n=34). The CD117$^+$ cells used for implantation were taken from the bone marrow of OsbY01 mice. A left thoracotomy without ligation of the left anterior descending artery was performed as a control (sham group, n=10).

Echocardiography

We assessed cardiac function before treatment and then 7, 14, 30, 60, and 90 days after treatment by echocardiography using a 7.5-MHz annular array transducer.[15,17] After the induction of light general anesthesia, the hearts were imaged 2-dimensionally in long-axis views at the level of the greatest left ventricular (LV) diameter. The systolic and diastolic LV areas were measured at the same time. This view was used to position the M-mode cursor perpendicular to the LV anterior and posterior walls. The LV end-diastolic diameters (LVEDDs) and LV end-systolic diameters (LVESDs) were measured from M-mode recordings according to the leading-edge method. The LV fractional shortening (%FS) was calculated as (LVEDD−LVESD)/LVEDD×100.

Histological Analysis

Five of the surviving mice from the preprogrammed and untreated groups were euthanized 30 or 60 days after treatment, and the remaining mice were euthanized 90 days after treatment. The hearts were harvested, and frozen sections 5 μm thick were used for histological analysis. The survival of implanted cells was detected by immunostaining with rabbit anti-GFP antibody (Molecular Probes) followed by FITC-conjugated goat anti-rabbit secondary antibody. Myogenic differentiation of surviving CD117$^+$ cells was identified by immunostaining with mouse anti-myosin, ventricular heavy chain α/β monoclonal antibody as described above.

To measure the microvessel density in the infarcted myocardium, sections were stained with anti-mouse CD31 antibody (Pharmingen). Capillaries were counted in 2 separate slides from at least 10 randomly selected fields under ×200 microscopy. The mean number

of capillaries per field in the infarcted myocardium was used for statistical analysis.

Azan staining was also performed to determine the wall thickness and the degree of collagen fiber accumulation in the infarcted region. By use of the image analysis software NIH IMAGE (NIH, Research Service Branch), the mean wall thickness was measured from 3 equidistant points, and the area of fibrosis was calculated as the area of stained fibrotic tissue divided by the total area of tissue. The measurements of wall thickness and area of fibrosis were performed on 2 separated sections of each heart, and the averages were used for statistical analysis.

Statistical Analysis

Data are expressed as mean±SD. Survival of animals was assessed by Kaplan-Meier analysis. Multiple-group comparisons were performed by ANOVA and Scheffé's test, using a significance level of $P<0.05$.

Results

TGF-β_1 Induced Myogenic Differentiation of CD117$^+$ Cells by Upregulating Expression of GATA-4 and Nkx2.5

After 7 days of culture with the supplement of 5 ng/mL TGF-β_1, ≈70% of the CD117$^+$ stem cells had a myoblast-like morphology under phase microscopy and were stained positively for myosin (Figure 1A), although ≈10% of these cells were also stained positively for myosin after 3 days of culture. However, they showed round and negative staining for myosin after 7 days of cultivation without the addition of TGF-β_1 (Figure 1A). Furthermore, RT-PCR analysis showed that the expression of several cardiac genes, β-myosin heavy chain, troponin I, troponin-T, and connexin-43, were also observed distinctly in these CD117$^+$ stem cells after 7 days of cultivation with 5 ng/mL TGF-β_1, but not without the addition of TGF-β_1 (Figure 1B).

Western blot analysis showed that the expression of GATA-4 and Nkx2.5 in these CD117$^+$ stem cells increased significantly after 1 and 3 days of cultivation with 5 ng/mL TGF-β_1, but not without the addition of TGF-β_1 (Figure 2). These results indicated that TGF-β_1 induced the myogenic differentiation of CD117$^+$ stem cells by the upregulation of GATA-4 and Nkx2.5 expression. Because 1 day of TGF-β_1 preprogramming was enough to induce myosin heavy chain expression after 7 days in vitro, we collected cells for implantation 1 day after cultivation with TGF-β_1.

A Low Concentration of TGF-β_1 Did Not Induce Osteoblast Differentiation of CD117$^+$ Cells

The ALP activity of CD117$^+$ stem cells increased to ≈1.5-fold that of newly isolated cells after 7 days of cultivation with 0, 1, and 5 ng/mL TGF-β_1, but this did not differ significantly according to whether 0, 1, or 5 ng/mL TGF-β_1 was added. However, the ALP activity increased to >10-fold after cultivation with 100 ng/mL TGF-β_1 (Figure 3A). Furthermore, immunostaining for osteocalcin showed that these CD117$^+$ stem cells were negative after 7 days of cultivation with 5 ng/mL TGF-β_1, but ≈10% were positive after 7 days of cultivation with 100 ng/mL TGF-β_1 (Figure 3B).

Regeneration of Injured Myocardium and Induction of Angiogenesis by the Implantation of Ex Vivo TGF-β_1–Preprogrammed CD117$^+$ Cells

Histological examination revealed that the implanted CD117$^+$ stem cells survived primarily in the scar and marginal region

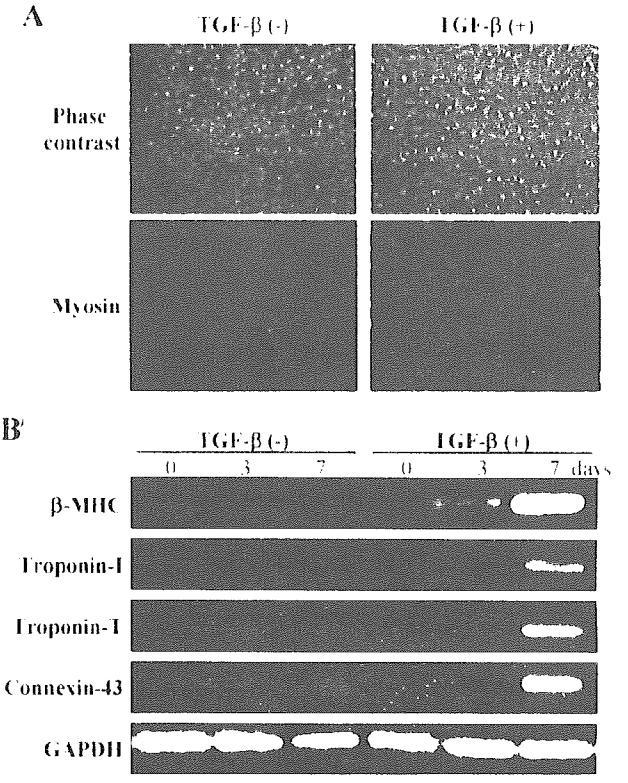

Figure 1. Myogenic differentiation of CD117$^+$ cells. A, Representative photomicrographs showed that many CD117$^+$ cells had a myoblast-like morphology and positive expression for myosin after 7 days of cultivation with 5 ng/mL TGF-β_1, but myosin-positive cells were not detected in CD117$^+$ cells cultivated without TGF-β_1. B, RT-PCR analysis of cardiac genes showed that CD117$^+$ cells distinctly expressed β-myosin heavy chain (β-MHC), troponin-I, troponin-T, and connexin-43 after 7 days of cultivation with TGF-β_1. However, these cardiac genes were expressed negative or very weakly in CD117$^+$ cells after 7 days of cultivation without TGF-β_1.

of infarcted myocardium in all mice from both the preprogrammed and untreated groups (Figure 4A). Most of the surviving CD117$^+$ stem cells were stained positively for myosin in the preprogrammed group, indicating the myogenic differentiation of programmed CD117$^+$ cells. However, myosin expression was rarely found in the untreated group. Quantitative analysis also showed that there were significantly more myosin-positive cells in the preprogrammed group than in the untreated group, although the total cell survival was similar in the 2 groups (Figure 4B). However, we did not observe positivity for osteocalcin in the grafted cells either.

A band of newly regenerated myocardium localized outside the scar tissue was observed in the preprogrammed group but not in the untreated group (Figure 5A). Although the wall thickness of the infarcted region was similar in the 2 groups, the area of fibrosis was significantly smaller in the preprogrammed group than in the untreated group (Figure 5B).

The mean microvessel count per field in the infarcted myocardium did not differ significantly between the preprogrammed and untreated groups (129.8±17.1 versus 138.2±20.5), but it was significantly higher in both the

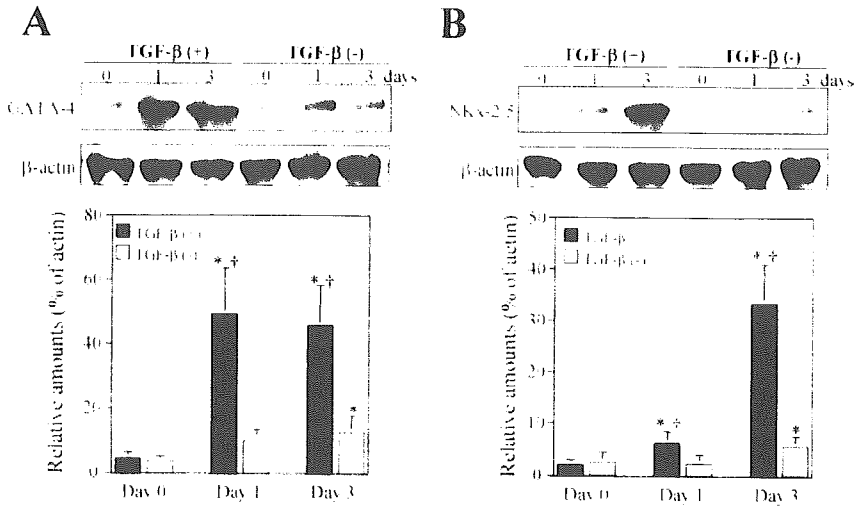

Figure 2. Expression of GATA-4 and Nkx2.5 in CD117$^+$ stem cells. Western blot analysis showed a significant increase in expression of GATA-4 (A) and Nkx2.5 (B) in CD117$^+$ cells after 1 and 3 days of cultivation with TGF-β_1. Quantitative analysis was derived from 5 independent experiments [*P<0.05 vs day 0 of same group, †P<0.05 vs TGF-β(-) group].

preprogrammed and untreated groups than in the PBS group (71.3±11.8, P<0.01; Figure 6). Although histological analysis was performed 30, 60, and 90 days after treatment, we presented the data only for 90 days after treatment, because the wall thickness and microvessel density did not change significantly within this time course.

Enhanced Cardiac Function After the Implantation of Ex Vivo TGF-β_1–Preprogrammed CD117$^+$ Cells

Although the technique of left anterior descending coronary artery ligation and intramyocardial injection was successful, ≈10% of the mice died of cardiac dysfunction soon after treatment. Within the 90 days of follow-up, 5, 8, and 13 mice from the preprogrammed, untreated, and PBS groups, respectively, died before they were scheduled to be euthanized. Statistical analysis showed that the survival rate was significantly higher in the preprogrammed group than in the PBS group (P<0.01), but the difference between the untreated and PBS groups was not significant (P=0.052, Figure 7).

Echocardiography showed that the motion of the LV anterior wall was obviously better in the sham, preprogrammed, and untreated groups than in the PBS group (Figure 8A). Quantitative analysis also showed that the %FS was significantly increased in the preprogrammed and untreated groups but not in the PBS group. Furthermore, the LV %FS was significantly higher in the preprogrammed group than in the untreated group after 2 weeks of treatment (Figure 8B).

Discussion

Bone marrow stem cells have the potential for both myogenic differentiation and the induction of therapeutic angiogenesis[6–8,14]; therefore, bone marrow is an important somatic stem cell source for functional myocardial regeneration. This study revealed a new physiological method of inducing myogenic differentiation of CD117$^+$ bone marrow stem cells by TGF-β preprogramming. Furthermore, functional regeneration of infarcted myocardium was effectively achieved by the intramyocardial implantation of TGF-β–preprogrammed CD117$^+$ bone marrow stem cells, related to either the regeneration of new myocardium or the induction of therapeutic angiogenesis.

It is well established that embryonic stem cells can be directed to differentiate into cardiomyocytes by signaling

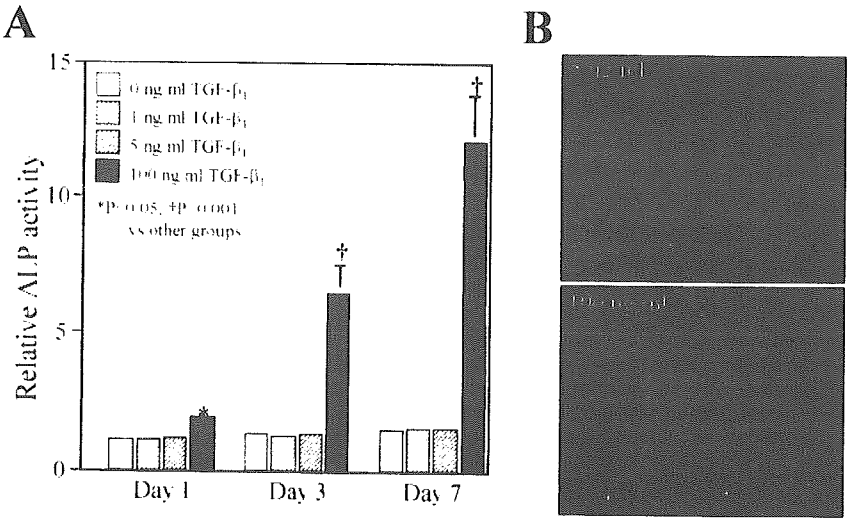

Figure 3. Osteoblast differentiation of CD117$^+$ cells. A, Quantitative analysis of data from 5 independent experiments showed that relative ALP activity of CD117$^+$ cells increased significantly after 3 and 7 days of cultivation with 100 ng/mL TGF-β_1 but not with concentrations of 1 and 5 ng/mL TGF-β_1. B, Immunostaining revealed positive staining for osteocalcin in ≈10% of cells after 7 days of cultivation with 100 ng/mL TGF-β_1 but not 5 ng/mL.

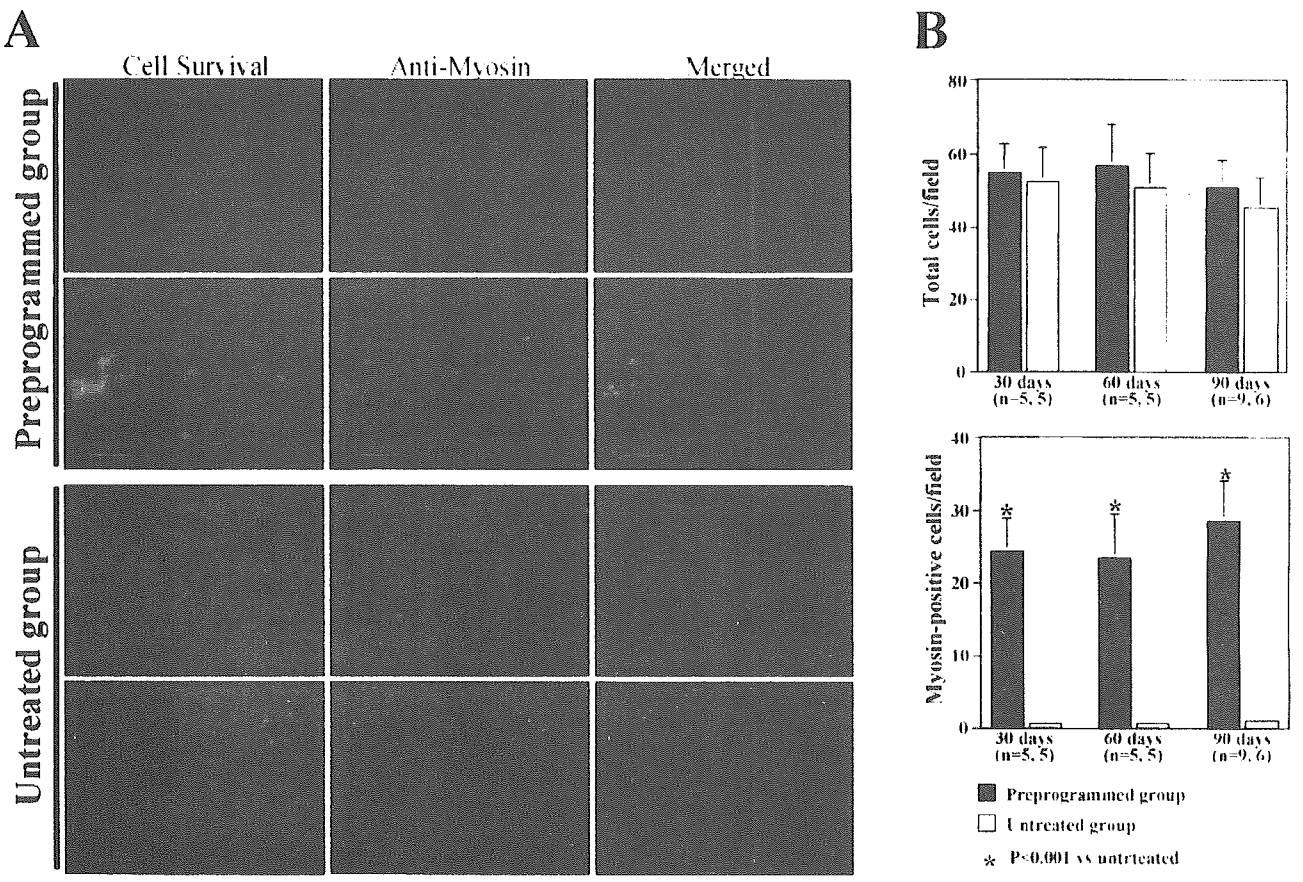

Figure 4. Myogenic differentiation of CD117$^+$ bone marrow stem cells in vivo. A, Representative cross section of infarcted myocardium 90 days after treatment. Note similar numbers of surviving implanted cells (green) in scar tissue of infarcted myocardium in preprogrammed and untreated groups (left). However, immunostaining revealed positive expression of myosin in TGF-β–preprogrammed CD117$^+$ cells but not in untreated CD117$^+$ cells after implantation (merged, right). B, Quantitative analysis showed that total cell survival did not differ significantly between preprogrammed and untreated groups but that there were significantly more myogenic differentiated (myosin-positive) CD117$^+$ cells in preprogrammed group than in untreated group.

through TGF-β/BMP2.[12] TGF-β can also induce the differentiation of neural crest stem cells into functional smooth muscle cells by the activation of Smad2 and Smad3 signaling pathways.[18] We found that TGF-β_1 could induce the myogenic differentiation of CD117$^+$ bone marrow stem cells in vitro, by upregulating the expression of GATA-4 and NKx-2.5 in CD117$^+$ bone marrow stem cells. This indicates that the signaling pathway mediated through TGF-β/BMP might play an important role in the myogenic differentiation of bone marrow stem cells. In fact, the myogenic differentiation in response to 5-azacytidine was also found to be partly dependent on *Bmpr1a*, a receptor for bone morphogenetic proteins.[19] However, the molecular mechanism responsible for TGF-β mediating these stem cells into myocytes and smooth muscle cells is still unclear.

Considering that TGF-β can induce osteoblast differentiation of bone marrow mesenchymal stem cells by mediation through the TGF-β/BMP-smad pathway,[20,21] it is possible that local calcification and bone formation within the myocardium might be induced by the intramyocardial injection of ex vivo TGF-β–preprogrammed CD117$^+$ bone marrow stem cells. Fortunately, TGF-β preprogramming by a concentration of 5 ng/mL or less did not significantly increase ALP activity or induce osteoblast differentiation of the CD117$^+$ cells in vitro or in vivo. However, osteoblast differentiation could be induced by a higher concentration of TGF-β.

Using the new physiological method of inducing myogenic differentiation of CD117$^+$ cells by TGF-β, we investigated the potential of functional cardiac regeneration by the intramyocardial injection of TGF-β–preprogrammed CD117$^+$ bone marrow stem cells. Although the intramyocardial implantation of CD117$^+$/Lin$^-$ bone marrow stem cells can regenerate infarcted myocardium effectively,[7] we separated the total CD117$^+$ bone marrow stem cells, because more than 80% of the separated CD117$^+$ cells are lineage-negative, and the remaining CD117$^+$/Lin$^+$ cells are considered a valuable subpopulation for inducing angiogenesis to improve regional perfusion in the infarcted myocardium.[11] In fact, the significant increase in microvessel density in our preprogrammed and untreated groups clearly demonstrated that the implantation of CD117$^+$ stem cells into the infarcted myocardium has the potential to induce therapeutic angiogenesis. This significant increase in microvessel density in both the preprogrammed and untreated groups contributed, at least in part, to

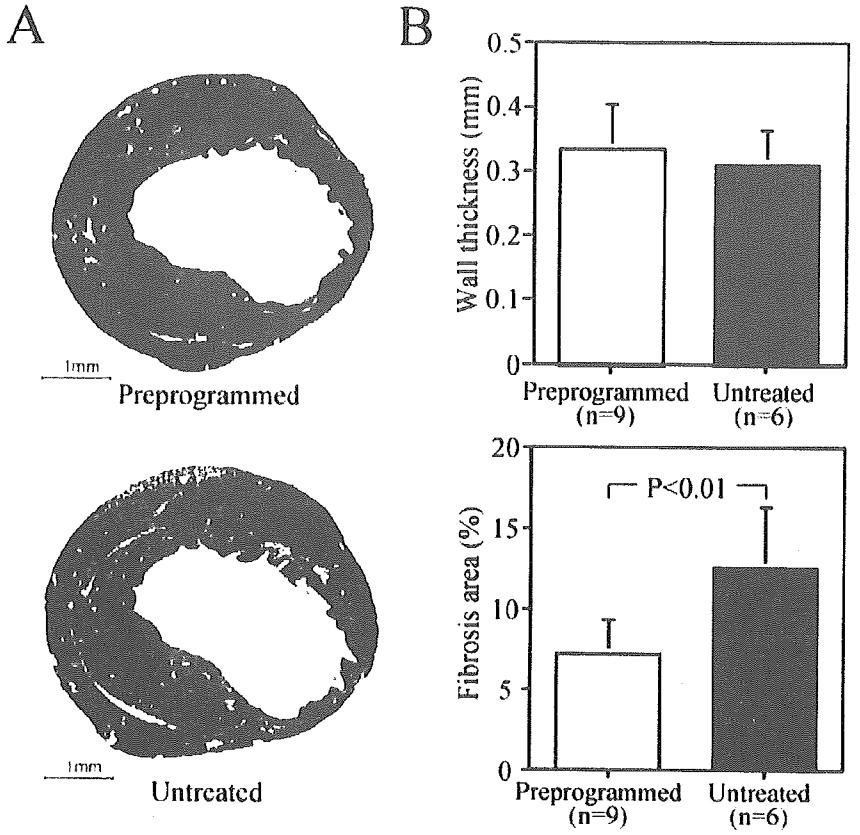

Figure 5. Azan staining of a cross section through infarcted myocardium 90 days after treatment. A, A band of newly regenerated myocardium (red line) was seen only outside scar tissue in preprogrammed group but not in untreated group. B, There was significantly more fibrous tissue in untreated group than in preprogrammed group, although wall thickness of infarcted region did not differ between 2 groups.

the improved cardiac function, which was also assisted by the injection of untreated CD117$^+$ stem cells, even though myocardial regeneration was not observed.

The fact that the LV %FS was significantly better in the preprogrammed group than in the untreated group indicates that more effective functional cardiac regeneration could be achieved by the implantation of TGF-β–preprogrammed cells than untreated cells. Although the cell survival seemed similar in the preprogrammed and untreated groups, many of the surviving CD117$^+$ cells in the preprogrammed group showed positive staining for myosin, whereas very few did in the untreated group. This indicates that 24 hours of TGF-β pretreatment improved the myogenic differentiation of CD117$^+$ cells implanted into infarcted myocardium. Furthermore, a band of newly regenerated myocardium was observed outside the scar tissue in the preprogrammed group, whereas fibrotic tissue was observed in the untreated group. Because the microvessel density was similar in the preprogrammed

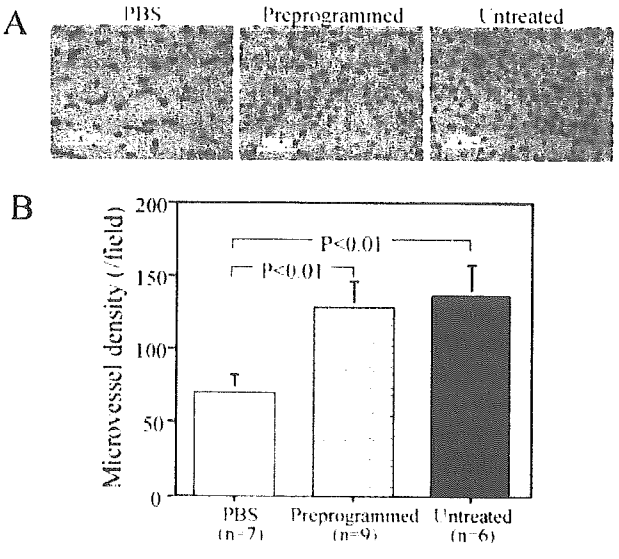

Figure 6. Microvessel density in infarcted myocardium 90 days after treatment. A, More microvessels were observed in preprogrammed and untreated groups than in PBS group. B, Quantitative analysis showed that microvessel density was significantly higher in preprogrammed and untreated groups than in PBS group, but it did not differ significantly between preprogrammed group and untreated group.

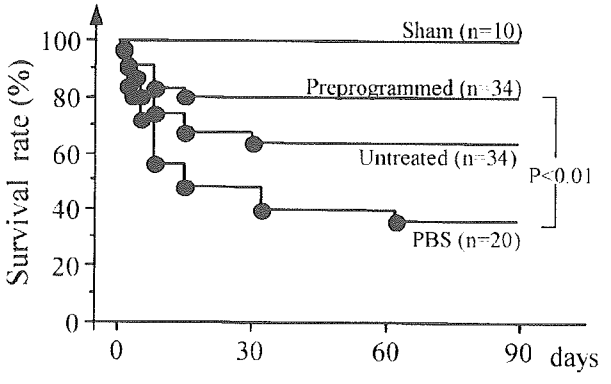

Figure 7. Cumulative percent survival of mice, plotted according to Kaplan-Meier method. Significance was analyzed with log-rank test.

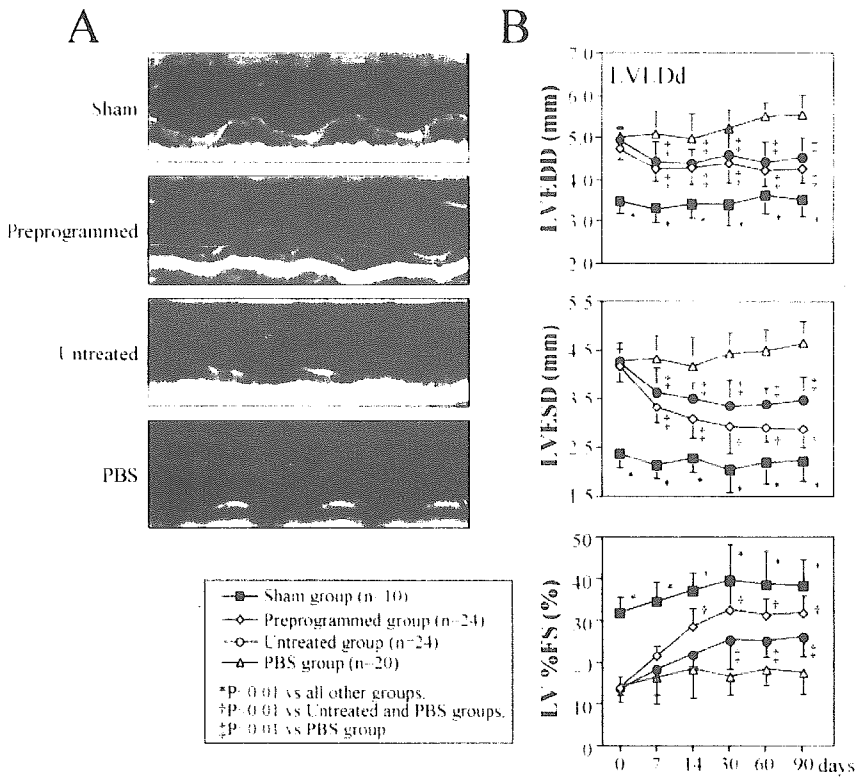

Figure 8. Echocardiographic assessment of cardiac function. A, Representative M-mode echocardiograms. B, Time course changes of FS%, LVEDD, and LVESD after treatment.

and untreated groups, we speculate that the enhanced functional cardiac regeneration achieved by the implantation of TGF-β–preprogrammed CD117$^+$ cells is related to the increased in situ myogenic differentiation from implanted cells and the decreased collagen fiber accumulation in the infarcted region.

A recent study by Beltrami and associates[22] showed that the myocytes produced by cardiac CD117$^+$ stem cells in infarcted myocardium are structurally and functionally competent, with normal contractile properties. Conversely, 2 very recent studies found that hematopoietic stem cells did not differentiate into cardiomyocytes in vivo.[23,24] There is still no consensus that the bone marrow stem cells can differentiate into cardiomyocytes. Our data show that untreated CD117$^+$ bone marrow stem cells rarely cause myogenic differentiation in vitro or in vivo. Although the myogenic differentiation of CD117$^+$ cells was increased dramatically by TGF-β preprogramming, we were unable to demonstrate that these myogenic differentiated CD117$^+$ bone marrow stem cells were really mature cardiomyocytes with normal contractile properties after implantation into infarcted myocardium.

Although TGF-β preprogramming favors the myogenic differentiation of CD117$^+$ bone marrow stem cells, we must identify the molecular mechanism of how TGF-β mediates stem cell differentiation into cardiomyocytes. Further studies must be conducted to search for direct evidence that these myogenic differentiated CD117$^+$ stem cells have normal contractile properties and contribute to improving cardiac function by forming synchronously beating networks around surviving host cardiomyocytes.

In conclusion, we found that adding a low concentration of TGF-β_1 induced the myogenic differentiation of CD117$^+$ stem cells by upregulating GATA-4 and NKx-2.5 expression. Therefore, the intramyocardial implantation of ex vivo TGF-β–preprogrammed CD117$^+$ bone marrow stem cells is a feasible method of functional cardiac regeneration, achieved by regenerating new myocardium through the in situ myogenic differentiation of implanted stem cells and by increasing regional perfusion through the induction of therapeutic angiogenesis.

Acknowledgments

This work was supported by a grant-in-aid for scientific research from the Ministry of Education, Science, Sports, and Culture (B16390397) and by a Research Grant for Cardiovascular Diseases (13C-1) from the Ministry of Health, Labor, and Welfare. We thank Mako Ohshima for excellent technical assistance.

References

1. Reinecke H, Zhang M, Bartosek T, Murry CE. Survival, integration, and differentiation of cardiomyocyte grafts: a study in normal and injured rat hearts. *Circulation*. 1999;100:193–202.
2. Soonpaa MH, Koh GY, Klug MG, Field LJ. Formation of nascent intercalated disks between grafted fetal cardiomyocytes and host myocardium. *Science*. 1994;264:98–101.
3. Li TS, Ito H, Kajiwara K, Hamano K. Long-term survival of xenografted neonatal cardiomyocytes by adenovirus-mediated CTLA4-Ig expression and CD40 blockade. *Circulation*. 2003;108:1760–1765.
4. Klug MG, Soonpaa MH, Koh GY, Field LJ. Genetically selected cardiomyocytes from differentiating embryonic stem cells form stable intracardiac grafts. *J Clin Invest*. 1996;98:216–224.
5. Taylor DA, Atkins BZ, Hungspreugs P, Jones TR, Reedy MC, Hutcheson KA, Glower DD, Kraus WE. Regenerating functional myocardium: improved performance after skeletal myoblast transplantation. *Nat Med*. 1998;4:929–933.
6. Tomita S, Li RK, Weisel RD, Mickle DA, Kim EJ, Sakai T, Jia ZQ. Autologous transplantation of bone marrow cells improves damaged heart function. *Circulation*. 1999;100(suppl II):II-247–II-256.

7. Orlic D, Kajstura J, Chimenti S, Jakoniuk I, Anderson SM, Li B, Pickel J, McKay R, Nadal-Ginard B, Bodine DM, Leri A, Anversa P. Bone marrow cells regenerate infarcted myocardium. *Nature*. 2001;410:701–705.
8. Makino S, Fukuda K, Miyoshi S, Konishi F, Kodama H, Pan J, Sano M, Takahashi T, Hori S, Abe H, Hata J, Umezawa A, Ogawa S. Cardiomyocytes can be generated from marrow stromal cells in vitro. *J Clin Invest*. 1999;103:697–705.
9. Ladd AN, Yatskievych TA, Antin PB. Regulation of avian cardiac myogenesis by activin/TGFβ and bone morphogenetic proteins. *Dev Biol*. 1998;204:407–419.
10. Zaffran S, Frasch M. Early signals in cardiac development. *Circ Res*. 2002;91:457–469.
11. Massague J. How cells read TGF-β signals. *Nat Rev Mol Cell Biol*. 2000;1:169–178.
12. Behfar A, Zingman LV, Hodgson DM, Rauzier JM, Kane GC, Terzic A, Puceat M. Stem cell differentiation requires a paracrine pathway in the heart. *FASEB J*. 2002;16:1558–1566.
13. Okabe M, Ikawa M, Kominami K, Nakanishi T, Nishimune Y. "Green mice" as a source of ubiquitous green cells. *FEBS Lett*. 1997;407:313–319.
14. Li TS, Hamano K, Nishida M, Hayashi M, Ito H, Mikamo A, Matsuzaki M. CD117+ stem cells play a key role in therapeutic angiogenesis induced by bone marrow cell implantation. *Am J Physiol*. 2003;285:H931–H937.
15. Nishida M, Li TS, Hirata K, Yano M, Matsuzaki M, Hamano K. Improvement of cardiac function by bone marrow cell implantation in a rat hypoperfusion heart model. *Ann Thorac Surg*. 2003;75:768–773.
16. Uchimura E, Machida H, Kotobuki N, Kihara T, Kitamura S, Ikeuchi M, Hirose M, Miyake J, Ohgushi H. In-situ visualization and quantification of mineralization of cultured osteogenetic cells. *Calcif Tissue Int*. 2003;73:575–583.
17. Tanaka N, Dalton N, Mao L, Rockman HA, Peterson KL, Gottshall KR, Hunter JJ, Chien KR, Ross J Jr. Transthoracic echocardiography in models of cardiac disease in the mouse. *Circulation*. 1996;94:1109–1117.
18. Chen S, Lechleider RJ. Transforming growth factor-β induced differentiation of smooth muscle from a neural crest stem cell line. *Circ Res*. 2004;94:1195–1202.
19. Oh H, Bradfute SB, Gallardo TD, Nakamura T, Gaussin V, Mishina Y, Pocius J, Michael LH, Behringer RR, Garry DJ, Entman ML, Schneider MD. Cardiac progenitor cells from adult myocardium: homing, differentiation, and fusion after infarction. *Proc Natl Acad Sci U S A*. 2003;100:12313–12318.
20. Qi H, Aguiar DJ, Williams SM, La Pean A, Pan W, Verfaillie CM. Identification of genes responsible for osteoblast differentiation from human mesodermal progenitor cells. *Proc Natl Acad Sci U S A*. 2003;100:3305–3310.
21. Moses HL, Serra R. Regulation of differentiation by TGF-β. *Curr Opin Genet Dev*. 1996;6:581–586.
22. Beltrami AP, Barlucchi L, Torella D, Baker M, Limana F, Chimenti S, Kasahara H, Rota M, Musso E, Urbanek K, Leri A, Kajstura J, Nadal-Ginard B, Anversa P. Adult cardiac stem cells are multipotent and support myocardial regeneration. *Cell*. 2003;114:763–776.
23. Balsam LB, Wagers AJ, Christensen JL, Kofidis T, Weissman IL, Robbins RC. Haematopoietic stem cells adopt mature haematopoietic fates in ischaemic myocardium. *Nature*. 2004;428:668–673.
24. Murry CE, Soonpaa MH, Reinecke H, Nakajima H, Nakajima HO, Rubart M, Pasumarthi KB, Virag JI, Bartelmez SH, Poppa V, Bradford G, Dowell JD, Williams DA, Field LJ. Haematopoietic stem cells do not transdifferentiate into cardiac myocytes in myocardial infarcts. *Nature*. 2004;428:664–668.

Journal of the American College of Cardiology
© 2005 by the American College of Cardiology Foundation
Published by Elsevier Inc.

Vol. 45, No. 12, 2005
ISSN 0735-1097/05/$30.00
doi:10.1016/j.jacc.2004.10.080

Detection of Lipid-Laden Atherosclerotic Plaque by Wavelet Analysis of Radiofrequency Intravascular Ultrasound Signals

In Vitro Validation and Preliminary In Vivo Application

Akihiro Murashige, MD, Takafumi Hiro, MD, PHD, Takashi Fujii, MD, PHD, Koji Imoto, MD, Takashige Murata, MD, Yusaku Fukumoto, MD, Masunori Matsuzaki, MD, PHD

Yamaguchi, Japan

OBJECTIVES This study examined the feasibility of using a wavelet analysis of radiofrequency (RF) intravascular ultrasound (IVUS) signals in detecting lipid-laden plaque.

BACKGROUND Wavelet analysis is a new mathematical model for assessing local changes in a geometrical profile of time-series signals.

METHODS Radiofrequency IVUS signals of 85 arbitrarily selected vectors were acquired from 27 formalin-fixed noncalcified atherosclerotic plaques from human necropsy with a digitizer at 500 MHz with 8-bit resolution by use of a 40-MHz IVUS catheter. Wavelet analysis of these RF signals was performed using a Daubechies-2 wavelet to obtain a color-coded map of the correlation coefficient with the wavelet reconstructed over the x-y plane of the wavelet scale and the distance from the IVUS catheter. The plaque segment was then examined histologically after being stained with Masson's trichrome stain. This technique also was applied in vivo in 29 human coronary plaque segments. These segments were excised subsequently by directional coronary atherectomy and processed for histologic analysis.

RESULTS In the in vitro study, histologic examination revealed lipid-laden segments in 29 vectors. When performing a wavelet analysis with the Daubechies-2 wavelet, the color-coded mapping revealed a different pattern in lipid-laden plaques compared with other types of plaque. Using this wavelet analysis, lipid-laden plaque could be detected with a sensitivity of 83% (24 of 29) and a specificity of 82% (46 of 56). In the in vivo study, fatty plaque could be detected with a sensitivity of 81% (13 of 16) and a specificity of 85% (11 of 13) with this method.

CONCLUSIONS Wavelet analysis of RF IVUS signals enabled in vitro as well as in vivo detection of lipid-laden plaque. This method may be useful in assessing plaque vulnerability in patients with coronary artery disease. (J Am Coll Cardiol 2005;45:1954–60) © 2005 by the American College of Cardiology Foundation

Because lipid-rich plaques with thin fibrous caps have been shown to be vulnerable to rupture as a major cause of acute coronary events (1,2), several attempts have been made to develop an imaging modality to identify such plaques before they rupture. Intravascular ultrasound (IVUS) imaging provides a detailed arterial cross section with accurate morphometric representation of atherosclerotic plaque dimensions in vitro and in vivo (3–15). However, subsequent studies have demonstrated significant limitations in tissue characterization by IVUS intensity patterns alone, especially in discriminating fibrous and fatty tissues (16–19). To overcome these limitations, many authors (19–24) have proposed methods of quantitative tissue characterization to discriminate fibrous and fatty plaque. However, none of these methods has been sufficiently well recognized as of yet for the appropriate equipment to be installed in commercially available IVUS machines.

See page 1970

Wavelet analysis is a new mathematical model for assessing local changes in the geometrical profile of time-series signals (25). Wavelet analysis is one of the time-frequency domain analyses of signals. This method discriminates a local unique wave pattern within a complex signal. The purpose of this study was to investigate the feasibility of using wavelet analysis of radiofrequency (RF) IVUS signals to detect lipid-laden plaque. The reliability of this method was first examined with in vitro atherosclerotic plaque segments from human necropsy. The parameters evaluated in this in vitro model were applied to an in vivo clinical setting and tested against the histology of the coronary segments excised with directional coronary atherectomy. The histology of the excised tissue was compared with the results of the wavelet analysis of RF IVUS signals.

From the Division of Cardiovascular Medicine, Department of Medical Bioregulation, Yamaguchi University Graduate School of Medicine, Yamaguchi, Japan. This work was partly supported by a grant-in-aid for scientific research of the Ministry of Education, Japan (grant No. 13670715). Health and Labour Sciences research grants: Comprehensive Research on Cardiovascular Diseases from Ministry of Health, Labour, and Welfare of Japan, and Knowledge Cluster Initiative of the Ministry of Education, Japan. This study was presented in part at the 75th scientific sessions of the American Heart Association, Chicago, Illinois, 2002. Drs. Murashige and Hiro contributed equally to this work.

Manuscript received June 13, 2004; revised manuscript received October 19, 2004, accepted October 25, 2004.

Abbreviations and Acronyms
IVUS = intravascular ultrasound
RF = radiofrequency

METHODS

In vitro IVUS study. Twenty-seven formalin-fixed noncalcified atherosclerotic plaques that were obtained from human femoral and coronary arteries excised from 10 patients at necropsy were imaged using a 40-MHz Atlantis Plus IVUS catheter (CVIS/Boston Scientific, Sunnyvale, California) in saline at room temperature. Eight of these patients died of heart failure with ischemic cardiomyopathy or old myocardial infarction, and two died of noncardiac events. The imaged arteries had plaques with a thickness >0.5 mm. The lumen area of the examine vessel was 10.48 ± 5.78 mm^2 (range, 1.57 to 25.2 mm^2).

Calcified plaques were not studied in the present study because calcified tissue is identified readily by visual inspection with high sensitivity and specificity (13). The current concern for tissue characterization of plaque is how to discriminate between fibrous and fatty tissue. An acoustic reference point was determined by suturing a surgical needle into the wall of the artery perpendicular to the long axis. This technique ensured that the same cross section was imaged for all studies and that the ultrasound images corresponded exactly to the cross section chosen for histologic analysis.

The entire length of the artery was imaged initially by visual inspection using conventional IVUS video monitoring to find an optimal portion of atherosclerotic plaque that provided no significant change in tissue composition or structure within at least a 0.5-mm length of the artery. Care was taken to position the catheter centrally and coaxially. The ultrasound images were recorded on super VHS tape.

Data acquisition. We sampled in vitro cross-sectional images of 27 noncalcified plaques in 21 atherosclerotic formalin-fixed artery specimens (coronary: n = 9; femoral: n = 12) with a commercially available IVUS machine (ClearView Ultra System, CVIS/Boston Scientific) and a 40-MHz IVUS catheter. The RF IVUS signals of 256 radial vectors, which completely surrounded (360°) the catheter center with an equal angle span (1.4°), were obtained from these plaques using an analog-to-digital converter installed inside the IVUS machine (Fig. 1). The analog-to-digital board was specially designed and installed by the IVUS manufacturer. Each cross section comprised these 256 RF IVUS signals, which were sampled in real time at 500 MHz in 8-bit resolution with a digitizer and then stored on hard disk for further analysis. Each cross-sectional IVUS image also was recorded on videotape. On a video screen, a radial line from the catheter center was superimposed on a conventional cross-sectional IVUS image to enable recognition of the location of each vector. The vectors analyzed were first obtained from the thickest portion of the plaque imaged. We next selected another two or more vectors at least 15 degrees away from the vector first selected. In other words, there were at least 10 vectors in between these vectors. Only the plaque portions, the thickness of which was more than 0.5 mm, were selected. The RF signals were excluded when the signals were from the regions with significant nonuniform rotational distortion, calcification, or drop-out in the conventional IVUS image. A total of 85 vectors were analyzed from all plaques imaged.

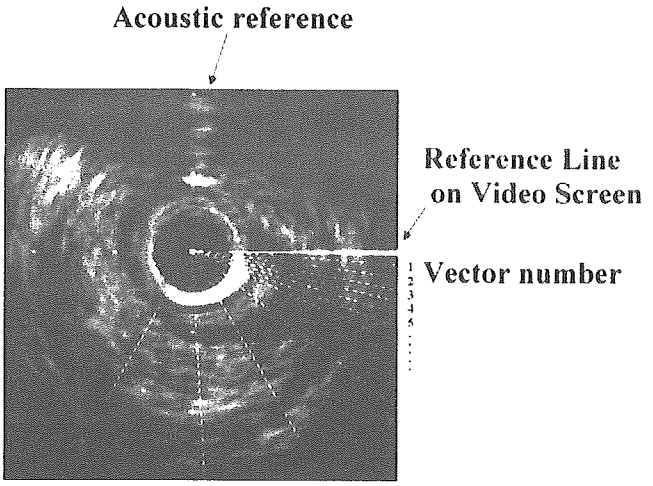

Figure 1. Acquisition of radiofrequency intravascular ultrasound signals. There are 256 radial vectors of radiofrequency signal sampled around the intravascular ultrasound catheter.

Wavelet analysis. We analyzed the IVUS RF signals offline by wavelet analysis (25) using MATLAB data processing software (The MathWorks, Natick, Massachusetts). Wavelet analysis is a signal-processing tool that enables the detection of a special geometric pattern within a localized area of a signal. A wavelet is a short segmental waveform of limited duration that has an average value of zero. Wavelet patterns that meet various mathematical

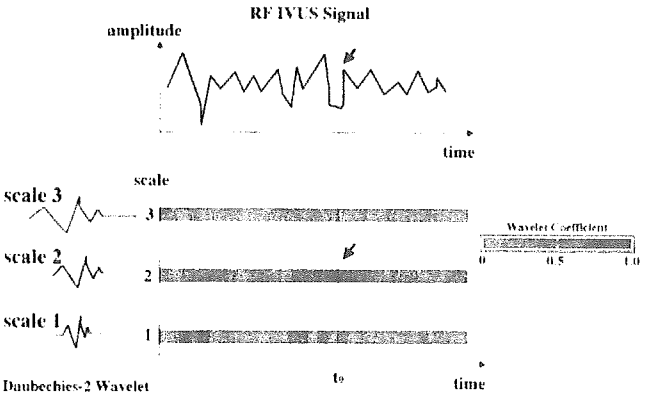

Figure 2. Procedure of wavelet analysis. In this example, a wavelet is stretched twice and three times. At a time of t0, a high value of wavelet coefficient is provided (**arrow**), suggesting that a special wave pattern similar to the wavelet of scale 2 is included within the signal at the time. IVUS = intravascular ultrasound; RF = radiofrequency.

JACC Vol. 45, No. 12, 2005
June 21, 2005:1954–60

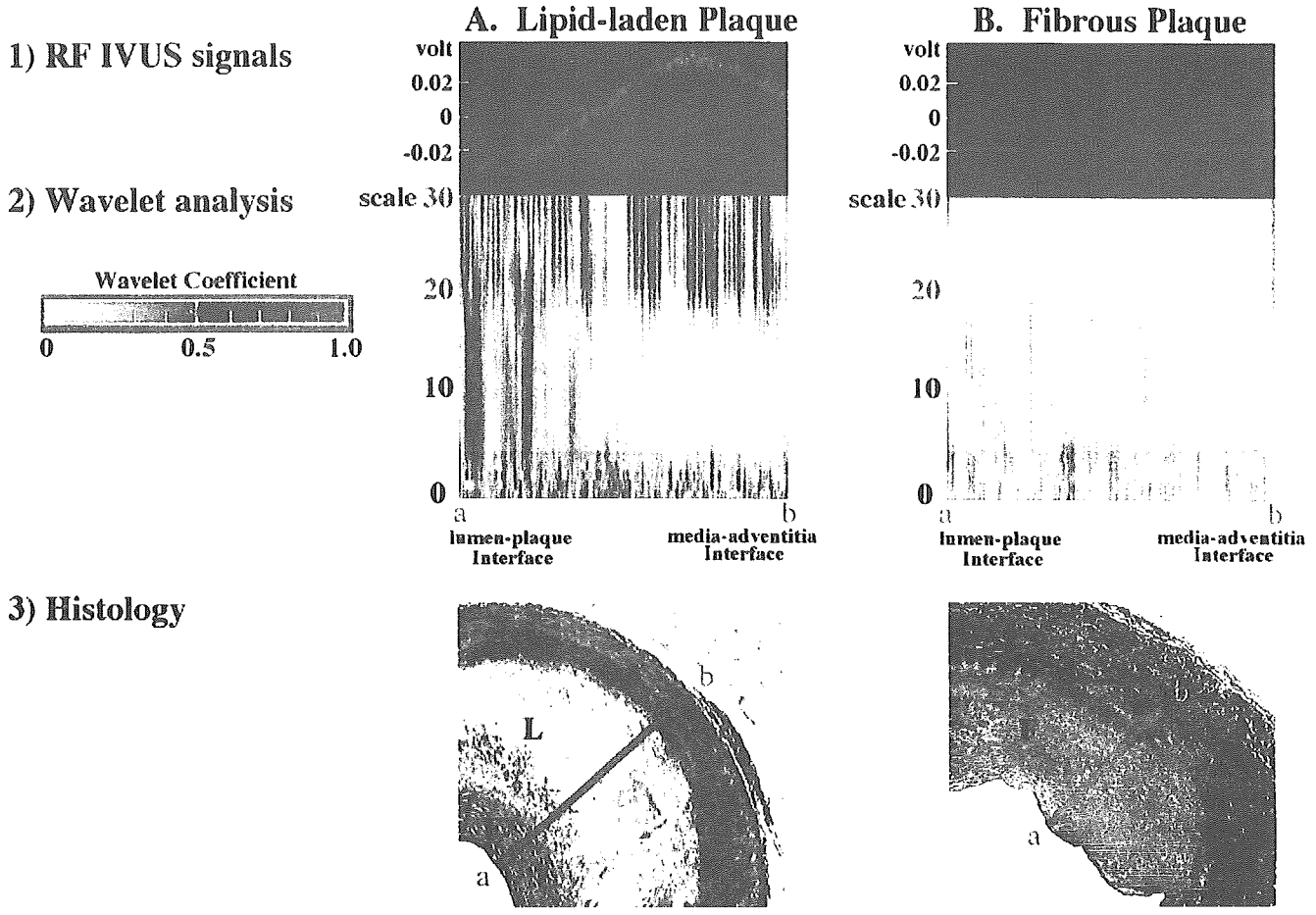

Figure 3. Representative examples of in vitro wavelet analysis of radiofrequency (RF) intravascular ultrasound (IVUS) signals from a lipid-laden plaque **(A)** and from a fibrous plaque without a lipid core **(B)**. The **upper panels** show RF signals, the **middle panels** show the results of wavelet analysis, and the **lower panels** show the histologic specimen of the corresponding arterial cross section with Masson's trichrome. In the time-scale domain color-coded mapping of wavelet analysis, an apparently different pattern of pink area from an RF signal vector of a lipid-laden plaque is observed between scale 20 and scale 30, compared with the fibrous plaque. F = fibrous area; L = lipid core.

criteria have been proposed for comparison, such as Daubechies, Meye, and Mexican hat. Wavelet analysis involves the breaking up of a signal into shifted and scaled versions of the original (or mother) wavelet. The continuous wavelet transform is defined as the sum over time of the signal multiplied by scaled, shifted versions of the wavelet function:

$$C(scale, position) = \int f(t)\Psi(scale, position, t)dt$$

This results in many wavelet coefficients, C, which are a function of scale and position. Multiplying each coefficient by the appropriately scaled and shifted wavelet yields the constituent wavelets of the original signal. Wavelet analysis then produces a time-scale view of a signal. "Scaling a wavelet" means stretching (or compressing) it. The greater the scale factor, the more the wavelet is stretched. This scale is related to the frequency of the signal. "Shifting a wavelet" simply means delaying (or hastening) its onset.

To obtain a wavelet analysis, the following steps are performed (Fig. 2)

1. Take a wavelet and compare it to a section at the start of the original signal.
2. Calculate C, the coefficient between the section and the wavelet, which represents how closely correlated the wavelet is with this section of the signal. The higher C is, the greater the similarity. The results will depend on the shape of the wavelet selected.
3. Shift the wavelet to the right and repeat steps 1 and 2 until the whole signal is covered.
4. Scale (stretch) the wavelet and repeat steps 1 through 3.
5. Repeat steps 1 through 4 for all scales.

This process produces wavelet coefficients (C) that are a function of scale and position. The commercially available program for wavelet analysis used in this study automatically selected the minimal scale of the wavelet to correspond to the minimum sampling interval.

After taking these steps, the coefficients are produced at different scales by different sections of the signal. The coefficients constitute a regression of the original signal performed on the wavelets. The results can be repre-

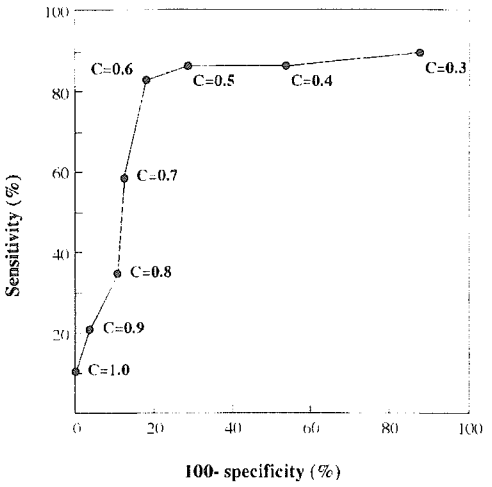

Figure 4. Receiver operating curve analysis was performed with varying degrees of the wavelet coefficient in terms of the capability of the in vitro detection of lipid-laden plaque. This analysis revealed that the optimal value of this wavelet coefficient to discriminate a lipid-laden plaque was 0.6. C = the wavelet coefficient.

sented graphically, in which the x-axis represents position along the signal (time), the y-axis represents scale, and the color at each x-y point represents the magnitude of the wavelet coefficient *C*. In this map, correlation coefficients are shown using a blue-pink scale, in which pink represents higher values of the coefficient and blue represents lower values.

Preliminary in vivo application. The same technique was applied in vivo to 29 coronary plaque segments from 13 patients (65 ± 6 years; range, 54 to 74 years) with coronary artery disease (7 patients with stable angina, 6 with acute coronary syndrome). The RF IVUS signals were obtained from the thickest part of the plaque imaged. These segments were excised by directional coronary atherectomy (FLEXI-CUT/Guidant, Indianapolis, Indiana) and processed for histologic analysis. Plaque segments were excluded, which were insufficiently debulked by the atherectomy, leaving a residual plaque area of more than one-third of the original plaque area. In the histologic preparation, the specimens were stained with hematoxylin-eosin stain and Azan stain. This study was approved by the institutional review committee, and patients gave informed consent.

Histologic study. In the in vitro study, after the arteries were imaged by IVUS, the needle for acoustic reference was removed, and the needle site marked with India ink. The specimens were processed for histology and stained with Masson's trichrome stain. The IVUS and the histologic examinations were performed by different observers. A plaque was defined as lipid-laden by visual inspection, when a lipid-core was >50% of the total plaque area. A lipid core was defined as a contiguous area of lipid-containing foam cells, extracellular lipids, cholesterol crystals, a lipid pool, or necrotizing material. A plaque was defined as fibrous when it had no distinct lipid core but had a fibroacellular matrix with dense collagen bands. The thickness of the lipid core had to be >0.3 mm and >50% of the total plaque area to be included in this study.

In the in vivo study, the directional coronary atherectomy specimens were stained with hematoxylin-eosin and Azan stains. This study only included typical fatty-dominant or fibrous-dominant plaques. The fatty-dominant plaques contained a lipid core >80% of total plaque area. The fibrous-dominant plaques contained a fibrous area >80% of total plaque area.

Statistical analysis. Values were expressed as means ± standard deviation. Receiver operating curve analysis was performed to discriminate the optimal criteria in the interpretation of the results of this wavelet analysis.

RESULTS

In vitro study. The mean thickness of plaque examined in this study was 1.42 ± 0.47 mm. Histologic examination revealed that 29 of 85 vectors of RF signals analyzed were from a lipid-laden plaque. Representative examples of wavelet analysis of RF IVUS signals from a lipid-laden plaque and from a fibrous plaque are shown in Figure 3. Wavelet analysis of the RF signals with a Daubechies-2 wavelet function provided an apparently different pattern in the color-coded mapping between scale 20 and scale 30. In this time-scale graphic representation of wavelet analysis of RF IVUS signals from a plaque with a lipid core, a different pattern of pink mapping was observed that was not observed from a fibrous plaque without a lipid core. A lipid-laden zone frequently was present, when the wavelet coefficient (*C*) was more than a certain value compared with a wavelet whose scale is between 20 and 30. The ROC analysis revealed that the optimal value of this wavelet coefficient was 0.6 to discriminate a lipid-laden plaque (Fig. 4). Using this criteria, the lipid-laden plaque was detected in this in vitro setting with a sensitivity of 83% (24 of 29) and a specificity of 82% (46 of 56) (Table 1). Many other wavelet approaches (approximately 50 types) were analyzed, and none provided the sensitivity and specificity of the Daubechies-2 method.

In vivo study. Histologic examination from the directional coronary atherectomies revealed that 16 of 29 coronary segments were fat-dominant (lipid-laden). No apparent fatty area was observed histologically in the remaining 13 segments. In the lipid-laden plaques, the wavelet analysis with the Daubechies-2 wavelet function revealed a similar

Table 1. Sensitivity and Specificity of Wavelet Analysis of Radiofrequency Intravascular Ultrasound Signals for Detecting Lipid-Laden Plaque

Histology		Wavelet Coefficient ≥0.6	Wavelet Coefficient <0.6
Lipid core (+)	in vitro (n = 29)	24/29 (83%)	5/29 (17%)
	in vivo (n = 16)	13/16 (81%)	3/16 (19%)
Lipid core (−)	in vitro (n = 56)	10/56 (18%)	46/56 (82%)
	in vivo (n = 13)	2/13 (15%)	11/13 (85%)

JACC Vol. 45, No. 12, 2005
June 21, 2005:1954–60

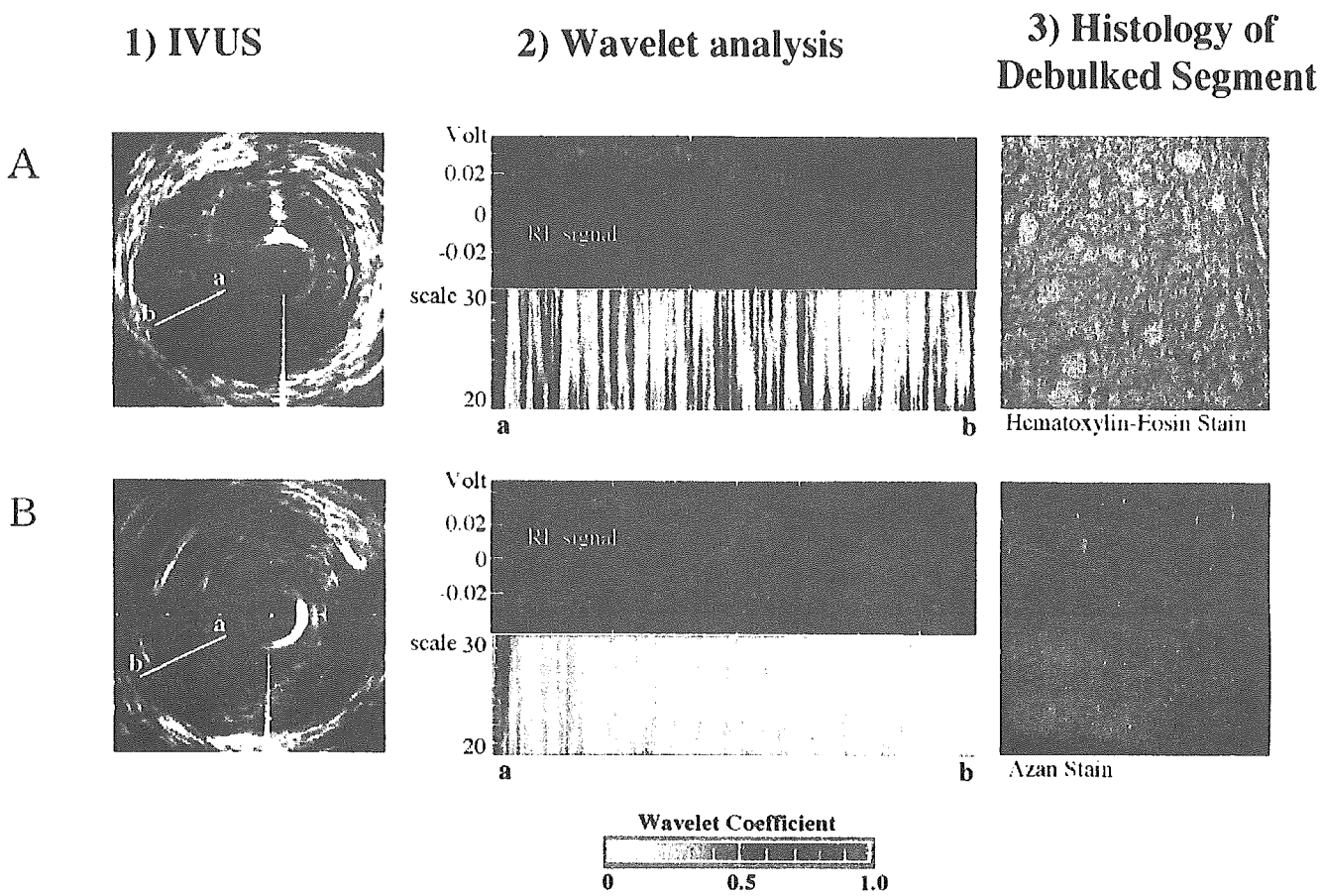

Figure 5. Representative examples of in vivo wavelet analysis of radiofrequency (RF) intravascular ultrasound (IVUS) signals from a lipid-laden plaque (**A**) and from a fibrous plaque without a lipid core (**B**). The **left panels** show conventional IVUS images, the **middle panels** show the results of wavelet analysis, and the **right panels** show the histologic cross sections of the corresponding directional coronary atherectomy specimen with hematoxylin-eosin and Azan stains. A similar pattern of color mapping was observed from the radiofrequency signal vector of a lipid-laden plaque, as seen in the in vitro study.

pattern as the in vitro results (Fig. 5). Using the same criteria of the wavelet analysis as in the in vitro study, fatty plaque could be detected from the clinical material with a sensitivity of 81% (13 of 16) and a specificity of 85% (11 of 13).

DISCUSSION

The present study is the first report of in vitro as well as in vivo tissue characterization of atherosclerotic plaque using a wavelet analysis of RF IVUS signals. The major finding of this study is that this wavelet method is accurate in detecting lipid-laden atherosclerotic plaque. This method may be useful in assessing plaque vulnerability in patients with coronary artery disease.

Advantages of wavelet analysis. The theoretical basis of wavelet analysis was first developed by Grossmann and Morlet in 1983 (25). Wavelet analysis is a time-frequency domain analysis of signals. The most well known of these is Fourier analysis, which breaks down a signal into constituent sinusoids of different frequencies. The Fourier transform was modified into a transform to analyze only a small section of the signal at a time by looking at "windows" of the signal. This short-time Fourier transform provides some information about when and at what frequencies a signal event occurs. The major drawback of this method is that once a particular size for the time window is chosen, that window is the same for all frequencies. If the window size is changed to a shorter one to increase time (space) resolution, the frequency resolution is compromised. Wavelet analysis was proposed in an attempt to overcome the problems in resolution.

Wavelet analysis represents a windowing technique with variable-sized regions. Wavelet analysis allows the use of long-time intervals when more precise low-frequency information is needed and shorter regions when high-frequency information is needed. One major advantage of wavelets is their ability to analyze a localized area of a larger signal. In this study, the Daubechies-2 wavelet proved best for detecting a lipid-laden plaque. An empirical selection of wavelet has to be made when applying wavelet analysis in a novel field of data. If a new wavelet family is developed, the sensitivity and specificity for detection of fatty tissue may be improved.

Wavelet scales 20 and 30 correspond to wavelengths of 32 and 47 μm, respectively. A scale of <20 is less than conventional IVUS resolution (26) or the ultrasound pulse

wavelength. The results from wavelet analysis with a wavelet scale <20 would measure artificial noise only. A higher value of wavelet correlation coefficient represents an acoustic signal derived from a more complicated structure. Compared with a fibrous area, a fatty area usually is composed of various kinds of tissue, such as lipid-laden foam cells, cholesterol crystals, extracellular lipids, necrotizing material, and fibers, which may be intermingled in a way that could produce complex acoustic impedance mismatches inside the plaque (17). Therefore, a lipid-laden area provides a higher value of wavelet correlation coefficient with a shorter scale of wavelet.

Comparison with other methods of tissue characterization. It was originally expected that tissue components within plaque could be identified from the video-intensity pattern of IVUS images (4,5,7,12–15). Subsequent studies, however, demonstrated significant limitations of tissue characterization by IVUS intensity patterns alone, especially in discriminating fibrous and fatty tissues or in assessing plaque vulnerability (16–19). To overcome the limitations, some authors (20–23) have proposed several methods of quantitative tissue characterization to discriminate fibrous and fatty plaque, including RF signal analysis, such as integrated backscatter analysis, attenuation slope mapping (19,24), and spectral analysis (27). Recently, IVUS elastography was proposed as a novel modality of tissue characterization with IVUS (28). Our laboratory previously reported that color mapping of the angle-dependent echo-intensity was useful for detecting fibrous caps within plaques (29). However, this method has difficulties in detecting other type of tissues. Because none of these previously reported techniques has become available commercially, no study has yet compared their clinical feasibility using the same subjects.

Study limitations. For the in vitro study, the arteries were imaged after they were fixed in formalin at room temperature. It is unknown whether formalin fixation or change in temperature will alter the results of this analysis. Another limitation was the use of nonpressure-distended arteries. When removed from physiologic pressure, atherosclerotic arteries contract. This contraction could significantly alter the architecture, which might affect the wave pattern of the RF IVUS signal. However, the in vivo application of the wavelet analysis also offered similar sensitivity and specificity for identifying a lipid-laden plaque as in the in vitro study. Therefore, these effects appear to be negligible in this study.

This wavelet analysis was performed for one single vector. The single vector analysis is subject to mismatch because of rotation of the images. To minimize any mismatch, we superimposed a radial line from the catheter center onto a conventional cross-sectional IVUS video image to enable the recognition of the location of each vector. In the in vitro study, all the plaques analyzed had a thickness >0.5 mm, and any lipid core had a thickness >0.3 mm. Therefore, we do not know whether it is possible to analyze thinner plaques or to identify very thin lipid cores with this method. Furthermore, the presence of blood and phasic pressure within the lumen as well as any noncoaxial alignment of the catheter may impair appropriate analysis in vivo with this method.

This study was performed on the off-line basis, taking an hour or so to obtain each color map. Therefore, a further development is necessary to be able to provide an on-line plaque evaluation during the study so that immediate feedback is given to the operator.

Conclusions. The present study demonstrates the feasibility of in vitro as well as in vivo tissue characterization by wavelet analysis of RF IVUS signals. Using wavelet analysis, lipid-laden plaque could be detected with a sensitivity and specificity of >80%. This method may be useful in assessing plaque vulnerability in patients with coronary artery disease. Currently, there is no reliable, commercially available device that is capable of discriminating fibrous and fatty areas within atherosclerotic plaque. Detection of vulnerable plaque or sequential observations of the stabilizing effect of lipid-lowering therapy on plaque composition with acceptable accuracy in vivo could improve the management of patients with coronary artery disease. Further evaluation of wavelet analysis in comparison with clinical data and inflammatory markers will be necessary to assess its usefulness in clinical practice to predict future cardiac events in patients with coronary artery disease.

Reprint requests and correspondence: Dr. Takafumi Hiro, Division of Cardiovascular Medicine, The Department of Medical Bioregulation, Yamaguchi University Graduate School of Medicine, 1-1-1 Minami Kogushi, Ube, Yamaguchi 755-8505, Japan. E-mail: thiro@yamaguchi-u.ac.jp.

REFERENCES

1. Fuster V, Badimon L, Badimon J, et al. The pathogenesis of coronary artery disease and the acute coronary syndromes. N Engl J Med 1992;326:242–50, 310–8.
2. Libby P. The molecular basis of the acute coronary syndromes. Circulation 1995;91:2844–50.
3. Yock PG, Johnson EL, Linker DT. Intravascular ultrasound: development and clinical potential. Am J Card Imaging 1988;2:185–93.
4. Gussenhoven EJ, Essed CE, Lancee CT, et al. Arterial wall characteristics determined by intravascular ultrasound imaging: an in vitro study. J Am Coll Cardiol 1989;14:947–52.
5. Tobis JM, Mallery J, Mahon D, et al. Intravascular ultrasound imaging of human coronary arteries in vivo. Analysis of tissue characterizations with comparison to in vitro histological specimens. Circulation 1991; 83:913–26.
6. Mallery JA, Tobis JM, Griffith J, et al. Assessment of normal and atherosclerotic arterial wall thickness with an intravascular ultrasound imaging catheter. Am Heart J 1990;119:1392–400.
7. Nissen SE, Grines CL, Gurley JC, et al. Application of a new phased-array ultrasound imaging catheter in the assessment of vascular dimensions: in vivo comparison to cineangiography. Circulation 1990; 81:660–6.
8. Potkin BN, Bartorelli AL, Gessert JM, et al. Coronary artery imaging with intravascular high-frequency ultrasound. Circulation 1990;81: 1575–85.
9. Nissen SE, Gurley JC, Grines CL, et al. Intravascular ultrasound assessment of lumen size and wall morphology in normal subjects and patients with coronary artery disease. Circulation 1991;84:1087–99.
10. Nishimura RA, Edwards WD, Warnes CA, et al. Intravascular ultrasound imaging: in vitro validation and pathologic correlation. J Am Coll Cardiol 1990;16:145–54.

11. Hodgson JM, Graham SP, Savakus AD, et al. Clinical percutaneous imaging of coronary anatomy using an over-the-wire ultrasound catheter system. Int J Card Imaging 1989;4:187–93.
12. Di Mario C, The SH, Madretsma S, et al. Detection and characterization of vascular lesions by intravascular ultrasound: an in vitro study correlated with histology. J Am Soc Echocardiogr 1992;5:135–46.
13. Friedrich GJ, Moes NY, Muhlberger VA, et al. Detection of intralesional calcium by intracoronary ultrasound depends on the histologic pattern. Am Heart J 1994;128:435–41.
14. Bartorelli AL, Potkin BN, Almagor Y, et al. Plaque characterization of atherosclerotic coronary arteries by intravascular ultrasound. Echocardiography 1990;7:389–95.
15. Peters RJ, Kok WE, Havenith MG, et al. Histopathologic validation of intracoronary ultrasound imaging. J Am Soc Echocardiogr 1994;7: 230–41.
16. Hiro T, Leung CY, Russo RJ, et al. Variability in tissue characterization of atherosclerotic plaque by intravascular ultrasound: a comparison of four intravascular ultrasound systems. Am J Card Imaging 1996; 10:209–18.
17. Hiro T, Leung CY, De Guzman S, et al. Are soft echoes really soft? Intravascular ultrasound assessment of mechanical properties in human atherosclerotic tissue. Am Heart J 1997;133:1–7.
18. Kimura BJ, Bhargava V, DeMaria AN. Value and limitations of intravascular ultrasound imaging in characterizing coronary atherosclerotic plaque. Am Heart J 1995;130:386–96.
19. Jeremias A, Kolz ML, Ikonen TS, et al. Feasibility of in vivo intravascular ultrasound tissue characterization in the detection of early vascular transplant rejection. Circulation 1999;100:2127–30.
20. Bridal SL, Fornes P, Bruneval P, et al. Parametric (integrated backscatter and attenuation) images constructed using backscattered radio frequency signals (25–56 MHz) from human aortae in vitro. Ultrasound Med Biol 1997;23:215–29.
21. Linker DT, Yock PG, Gronningsaether A, et al. Analysis of backscattered ultrasound from normal and diseased arterial wall. Int J Card Imaging 1989;4:177–85.
22. Kawasaki M, Takatsu H, Noda T, et al. Non-invasive tissue characterization of human atherosclerotic lesions in carotid and femoral arteries by ultrasound integrated backscatter: comparison between histology and integrated backscatter images before and after death. J Am Coll Cardiol 2001;38:486–92.
23. Kawasaki M, Takatsu H, Noda T, et al. In vivo quantitative tissue characterization of human coronary arterial plaques by use of integrated backscatter intravascular ultrasound and comparison with angioscopic findings. Circulation 2002;105:2487–92.
24. Wilson LS, Neale ML, Talhami HE, et al. Preliminary results from attenuation-slope mapping of plaque using intravascular ultrasound. Ultrasound Med Biol 1994;20:529–42.
25. Daubechies I, Grossmann A. An integral transform related to quantization. J Mat Phys 1980;21:2080–90.
26. Benkeser PJ, Churchwell AL, Lee C, et al. Resolution limitations in intravascular ultrasound imaging. J Am Soc Echocardiogr 1993;6: 158–65.
27. Nair A, Kuban BD, Tuzcu EM, et al. Coronary plaque classification with intravascular ultrasound radiofrequency data analysis. Circulation 2002;106:2200–6.
28. de Korte CL, Sierevogel MJ, Mastik F, et al. Identification of atherosclerotic plaque components with intravascular ultrasound elastography in vivo: a Yucatan pig study. Circulation 2002;105: 1627–30.
29. Hiro T, Fujii T, Yasumoto K, et al. Detection of fibrous cap in atherosclerotic plaque by intravascular ultrasound by use of color mapping of angle-dependent echo-intensity variation. Circulation 2001;103:1206–11.